This information product has been peer reviewed and approved for publication by the U.S. Geological Survey

Novel Adomaviruses Associated with Blotchy Bass Syndrome in Black Basses (*Micropterus spp.)*

Luke R. Iwanowicz[1,2*], Clayton D. Raines[2], Kelsey T. Young[3], Vicki S. Blazer[2], Heather L. Walsh[2], Geoff Smith[4], Cynthia Holt[5], John Odenkirk[6], Tom Jones[7], Jan-Michael Hessenauer[8], Morgan A. Biggs[2], Christopher B. Buck[9], Justin Greer[10] and R. Scott Cornman[11].

1 – U.S. Department of Agriculture/Agriculture Research Service, National Center for Cool and Coldwater Aquaculture, Kearneysville, WV

2 - U.S. Geological Survey, Eastern Ecological Science Center, Kearneysville, WV

3 - Pennsylvania Department of Agriculture, Pennsylvania Veterinary Laboratory, Harrisburg, PA

4 - Pennsylvania Fish and Boat Commission, Bellefonte, PA

5 - Texas Parks and Wildlife Department, Fort Worth, TX

6 - Virginia Department of Wildlife Resources, Fredericksburg, VA

7 - Vermont Fish & Wildlife Departments, Montpelier, VT

8 - Michigan Department of Natural Resources, Harrison Twp, MI

9 - National Cancer Institute, Bethesda, MD

10 - U.S. Geological Survey, Western Fisheries Science Center, Seattle, WA

11 - U.S. Geological Survey, Fort Collins Science Center, Fort Collins, CO

[*] Corresponding author

Email: luke.iwanowicz@usda.gov

Abstract

Black bass (*Micropterus spp.*) are the most important warmwater game fishes in the United States. They have high socioeconomic and recreational value and support an important aquaculture industry. Since 2008, fisheries managers have been reporting the observation of hyperpigmented melanistic lesions (HPMLs) on smallmouth bass (*M. dolomieu*) in different ecoregions of the United States. Similar HPMLs have been observed in largemouth bass (*M. nigricans*) since the 1980's. Here, we report a close association between novel adomaviruses and the hallmark blotchy clinical presentation of hyperpigmented lesions on the skin smallmouth and largemouth black bass and provide evidence that satisfies Rivers' postulates. The two adomaviruses are structurally and phylogenetically similar but share only 68.0% identity at aligned nucleotide sites and each has been found in only one host species to date. The manifestation of this skin disease appears to be seasonal in both species, primarily affects adults and is of unknown health consequence. Although the significance of infection to fish health remains unclear, understanding the disease ecology of these can inform biosecurity and the interjurisdictional movement of individuals. Moreover, as hyperpigmentation in other fish species is often idiopathic, our findings reframe perspectives for future investigations into this clinical presentation in other species.

Introduction

Black bass (*Micropterus spp.*) are iconic North American sportfishes that support the most economically valuable freshwater sport fishery in the United States [1]. They are associated with a multibillion-dollar industry annually represented by recreational angling and aquaculture [2, 3]. Black bass are keystone predators within freshwater ecosystems and represent the most prized warmwater recreational sportfish in North America [4]. While indigenous to North America, largemouth bass (*M. nigricans,* LMB) and smallmouth bass (*M. dolomieu,* SMB) now have a cosmopolitan distribution as they have been introduced throughout the world due to their desirability as a sportfish [5]. Broodstock for black basses are maintained for private and public stocking. In addition, LMB production as a food fish is an emerging market in the United States and part of a thriving aquaculture industry in Asia [3, 6].

Between 2003 and 2010 there was an increased frequency of mortality events, low relative abundance, and poor year classes of SMB in specific areas of the Susquehanna and Potomac River Basins of the eastern United States [7, 8]. Coincident with these reports were increased observations of macroscopic lesions of the integument associated with opportunistic microbes [9]. These prolonged mortality events drew public attention to fish and ecosystem health. Notably, as these widespread mortality events abated in the Susquehanna River system during the latter end of this timeline (ca. 2010), hyperpigmented melanistic skin lesions (HPMLs) in SMB previously unreported in this watershed were increasingly observed with a springtime prevalence as high as 55% [10]. Interestingly, fisheries managers started observing or receiving reports of HPMLs on SMB in disparate watersheds in the United States around this same time (Lake St. Clair, MI in 2008, Lake Champlain, VT in 2009; rivers of the Great Lakes Region in 2010; Potomac River, WV in 2012)[10, 11]. The appearance of HPMLs among black

bass has become so commonplace that the condition is colloquially referred to as "blotchy bass syndrome" (BBS) by anglers and resource managers. The first official report of BBS in LMB dates to a case in 1984 from the Hudson River, NY (S1 Fig) [12]. Although anecdotal evidence suggests sporadic observations of BBS in LMB for the last 40 years or more, documented accounts primarily exist in online message boards, angler-supported social media resources, or non-interpretive reports [13].

HPMLs associated with the integument have been reported in marine and freshwater fishes worldwide [10, 14-18]. These lesions often manifest as macroscopic, discrete, focal or multifocal areas of hypermelanization on the external surface of the fish. Histological descriptions of these lesions typically include an atypical increased density of melanocytes within the epidermal and dermal strata of the skin, disruption of the basement membrane, or pleiomorphic cell morphology [15, 19]. Other than black spot disease that is caused by parasitic infections in fishes and is clinically distinguishable from BBS, modest efforts have been made to identify the etiology of HPMLs [20-22]. Diagnostic analysis including histopathology, culture-based virology, molecular and classical bacteriology and electron microscopy have been attempted to identify putative microbial agents in many other instances; however, such lesions are typically idiopathic in nature. Hypermelanization has been ascribed to possible exposure to environmental contaminants, exposure to ultraviolet radiation or other unspecified environmental stressors, or genetics, yet there is a paucity of experimental evidence to support these candidate causes [14, 23].

Despite nearly a half century of BBS observations in black basses, little progress has been made to resolve the etiology of this idiopathic syndrome. We recently found evidence of a putative adomavirus associated with HPMLs in SMB [10]. To shed further light on a possible

causal relationship, we searched for similar viruses in LMB with HPMLs. Here, we present complete genomes of two phylogenetically related, but clearly different species of adomaviruses associated with the HPMLs hallmark of BBS and provide phylogenetic evidence that the emergence of this disease in SMB may not be the result of recent introductions.

Materials and Methods

Specimen Sampling

All live animal handling and use procedures were reviewed and approved by the U.S. Geological Survey, Eastern Ecological Science Center Animal Care and Use Committee (IACUC 07001, 2020-06 and 2021-17L). Samples were acquired from both LMB and SMB from a variety of natural aquatic settings including the Susquehanna River Basin (PA), the Potomac River Basin (VA), Lake St. Clair (MI), Lake Champlain (VT) and western Texas. Alternatively, fish maintained in aquatic exhibits at Bass Pro Shops and Cabela's with HPMLs were sampled (S1 Table).

Most of the samples utilized for this research were collected with non-lethal, minimally invasive approaches. Archived samples collected from tandem research efforts in 2017 and 2019 were also used [10, 24, 25] . Those fish were euthanized with an overdose of tricaine methanesulfonate (MS-222, Argent Labs, Redmond, WA). Otoliths were removed for ageing and phenotypic sex was determined in lethally sampled fishes. Age and sex could not be determined for non-lethally sampled individuals. Depending on the sample, clinically affected or normal scales were collected for analysis, and nucleic acids were preserved in RNA*later* (Thermo Fisher Scientific, Waltham, MA) or DNA/RNA Shield (Zymo Research, Irvine, CA). Most non-lethal sampling included the use of swabs and collection tubes containing DNA/ RNA Shield. The HPMLs or normal skin were sampled by rubbing the swab back and forth with gentle, yet firm

pressure for 10-15 seconds. The swab head was then rotated such that the entire surface contacted the sample area. Transfer of melanin to the swab confirmed tissue transfer in the case of HPMLs (S1 Video). Swabs were then inserted in the collection tube for subsequent nucleic acid extraction. Details regarding specific methods are provided as supplemental material (S1 Text)

Nucleic acid extraction, sequencing and *de novo* assembly of viral genomes

Nucleic acid extraction, sequencing and *de novo* assembly methods differed across the sample sets utilized for downstream analysis and are included as supplemental materials (S1 Text).

Identification of virus positive samples and resolving repetitive regions

PCR primers were designed to amplify a loci of the RepE1 gene in each virus. The forward primers were anchored in the parvovirus non-structural protein NS1 conserved domain for MdA-1 and MnA-1 to minimize the likelihood of target sequence mismatch across samples given uncertainly in sequence variability. Primers were designed using the modified version of Primer3 2.3.7 bundled within Geneious Prime v2020.0.5 [26]. Primer sequences are listed in Table 1. Conventional PCR was conducted as 25 µl reactions consisting of 1 µl of unquantified DNA template, 400nM of primers in GoTaq Green master mix (Promega, Madison, WI). Thermal-cycling profiles were as follows: denature at 95ºC for 3 min then 30 cycles of 95ºC for 30 s, 60ºC for 40 s, and 72ºC for 60 s. Final extension at 72º for 5 minutes. Final hold at 4ºC. The product size is indicated in the primer name. A subset of RepE1 products PCR products were purified using a QIAquick PCR Purification Kit (Qiagen, Hilden, Germany) and confirmed via Sanger sequencing.

Table 1. Primers and thermal cycling conditions for the amplification of bass adomavirus helicase genes.

Primer	5'-3'	RepE1 (genome coordinates)
MdA-1_EO1F779	CACAGTGCTGCATTGCTTGT	13,517 – 14,295
MdA-1_EO1R779	CTTGATGCATGTGACTCGCG	
MnA-1_EO1F851	TCTCTCAGAGACCGGTTCGT	13,556 – 14,406
MnA-1_EO1R851	TGCTCGTGCCCTTAACAGAG	
MdA-2_EO1F718	AAATGGGCAGCACAGCAAAG	16,083 – 16,800
MdA-2_EO1R718	AATGACAGAGTTCGCAGGCA	

All PCR was conducted as 25 µl reactions consisting of 1 µl of unquantified DNA template, 400nM of primers in GoTaq Green master mix (Promega, Madison, WI). Thermal-cycling profiles were as follows: denature at 95ºC for 3 min then 30 cycles of 95ºC for 30 s, 60ºC for 40 s, and 72ºC for 60 s. Final extension at 72º for 5 minutes. Final hold at 4ºC. The product size is indicated in the primer name.

Comparison of adomaviruses from large and smallmouth bass

Complete genomes of the black bass adomaviruses were ordinated such that the linearized sequence terminated at the beginning of the SET ORF. Open reading frames were predicted using Geneious Prime. Candidate protein sequences without clear hits via BLASTP were analyzed with HHpred using the NCBI Conserved Domains, PDB_mmCIF70, Pfam-A, and UniProtSwissProt-viral70 databases [27]. Sequences without clear hits in HHpred searches were queried via Dali using predicted protein structure from AlphaFold2 or RoseTTAfold predictions [28-30]. In some instances, we assigned protein names based on synteny even when not supported by prediction queries as not to further infer function in the absence of experimental data [31, 32].

Genomes were aligned using MUSCLE v5.1 bundled with Geneious Prime software v2024.0.2 to determine pairwise identity [33]. All homologous proteins were aligned to determine protein identity in a similar fashion.

Visualizing viral nucleic acid (RNAscope)

In order to visualize viral nucleic acids in HPMLs we developed an *in situ* hybridization RNAscope® assay that utilized a 15ZZ probe targeting nucleotides 4 - 778 of the MdA-1 adenain gene (UFQ21633). A 12ZZ probe targeting nucleotides 2 – 684) of the MnA-1 adenain gene (XQZ12369) was also developed. Because of the small, low complexity dsDNA genome, this probe effectively targets both viral mRNA and genomic DNA. We analyzed SMB samples from a health assessment study in the Susquehanna River, PA collected during fall 2013 and spring 2024 [24, 34]. Samples from LMB were collected from Raystown Lake, PA during the spring of 2024. Normal skin tissue as well as skin with HPMLs stabilized in PAXgene® Tissue FIX (PreAnalytiX, Switzerland) were decalcified with 0.5M EDTA for 48 hr, embedded into paraffin, and sectioned at 5 µm. RNAscope (Advanced Cell Diagnostics, Newark, California) was used to observe the localization of the target gene nucleic acids. Selected sections with HPMLs were deparaffinized with three changes of Pro-Par clearant (Anatech Ltd., Michigan) for 5 min each and rehydrated with a graded ethanol series of 100%, 95%, 80%, 70%, and 50% for 3 min each and air dried. RNAscope was conducted according to the manufacturer's protocols for the RNAscope Multiplex Fluorescent Reagent Kit v2 Assay. The RNAscope Protease Plus incubation step was omitted given that assay optimization identified that PAXgene preserved samples were overly digested. The target probes were heated to 40°C for 10 min, cooled to room temperature and hybridization was carried out at 40°C for 2 h in an InSlide Out hybridization oven (Boekel, Pennsylvania). A negative control consisted of the probe diluent only. Sample controls included normal no HPML) skin. Slides were counterstained with Sudan Black B for 30 s, rinsed clear with deionised water and mounted with ProLong Gold Antifade Mountant (Thermo Fisher Scientific, Carlsbad, California). Slides were imaged with a Keyence BZ-X810 (Itasca, IL). Fluorescent signal from viral nucleic acids was visualized (ex: 470 $\pm$ 40nm; em: 525

± 50nm). Digital images were imported into GIMP 2.10.32 to construct composite figures and correct for autofluorescence [24].

Viral gene expression (RNA-seq)

We evaluated the expression of viral transcripts in HPMLs of smallmouth bass collected in 2017 (BioProject PRJNA530557) and 2022 (BioProject PRJNA1254126) as well as largemouth bass collected in 2022 (BioProject PRJNA1253685). Adapter removal and quality control of the raw sequencing reads was performed in trimmomatic with the parameters set as LEADING:5 TRAILING:5 SLIDINGWINDOW:4:15 MINLEN:25. Cleaned reads passing quality control were first aligned to the host transcriptome obtained from the NCBI (LMB: accession GCF_014851395.1_ASM1485139v1, SMB: accession GCF_021292245.1_ASM2129224v1) to remove reads originating from the host. Reads were aligned to the appropriate transcriptome using salmon (v1.4.0) in mapping mode with GC bias and selective alignment [35]. Parameter settings were maintained for both paired-end (2022) and single-end (2017) sequencing datasets. Reads that did not align to the host transcriptome were obtained using –writeUnmappedNames in salmon followed by sequence extraction using subseq from the seqtk package [36]. These reads were then aligned all non-overlapping ORFs of MdA-1 or MnA-1 using salmon to quantify the abundance of viral transcripts.

Viral transcript quantification was imported into R using tximport and counts were normalized in DESeq2 using the counts function with normalized = TRUE [37, 38]. Viral transcripts were not detected in clinically normal fish or regions not presenting hyperpigmented lesions and these samples were therefore removed prior to downstream visualization in order to appropriately calculate dispersion and count variance.

Phylogenetic analysis

We recovered adomavirus protein sequences of the replicase gene (RepE1, RepLT or CressRep), Adenain, and Hexon from NCBI (S2 Table). Sequences were aligned using MUSCLE v5.1 bundled within Geneious Prime software v2024.0.2 [33]. Alignment files were used to infer phylogenetic trees in IQ-Tree 1.6.12 for each of the viral proteins [39]. Phylogenetic trees were visualized using iTOL v6 [40]. Pairwise identity of translated amino acid sequences for these proteins were determined and visualized using the Sequence Demarcation Tool [41].

Results

Gross presentation of blotchy bass syndrome and site-specific prevalence

The HPMLs observed on both bass species investigated here shared an indistinguishable gross presentation (Fig 1). These areas of hyperpigmentation presented on the external surface of fish including the fins and margins of the oral cavity. Lesions consisted of sharply circumscribed, melanistic macules of variable size with irregular, asymmetric borders surrounded by normal-appearing skin. The gross morphology of discrete, melanistic blotches was visually suggestive of melanin irregularly radiating from a central focal point. In some instances, these blotches coalesced into more intricate, amorphous patterns. Of note, during the late spring these HPMLs were often fragile and the integument in these focal areas was disrupted with gentle pressure (S1 Video). HMPL fragility was not observed in the fall. Gross and histological descriptions in SMB have been reported previously [10].

Comprehensive size-distribution surveys of SMB were initiated in Lake St. Clair, MI during 2002. These surveys were always conducted during May prior to spawning. In 2008 the hallmark presentation of BBS was first observed at a frequency such that fisheries managers

began documenting this external anomaly (Fig 2A). Since 2008, the prevalence of blotchy SMB ranged from 1.7 - 9.2% ($\bar{x}$=5.1%; n=5,893). These surveys primarily targeted adults (180 - 560mm) and the smallest blotchy bass was 320 mm. Although blotchy LMB are observed in Lake St. Clair, a similar prevalence dataset is not available.

The Virginia Department of Wildlife Resources performed mark-recapture surveys between March and April 2021 to estimate LMB population size structure across 7 tributaries in the Potomac River Watershed. The prevalence of BBS was also documented during this pre-spawn sampling. Blotchy LMB were observed at all sample locations (Fig 2B). The smallest blotchy fish was 278 mm. Prevalence of blotchy LMB ranged from 4.3 - 23.0% ($\bar{x}$=16.2%; n=470).

Association of adomaviruses with HPMLs

Initial transcriptome assemblies generated during a previous study identified a papillomavirus helicase-like sequence (MT010627) in HPMLs of SMB, motivating additional DNA sequencing to complete a reference genome (10). The genome model presented here proposes a circular dsDNA of 16,002 bp (MZ673484) with gene content and phylogenetic position consistent with other fish-associated adomaviruses (S2 Fig). We refer to this virus as *Micropterus dolomieu adomavirus 1* (MdA-1). In addition, a variant of MdA-1 was recovered from DNA sequencing of an HPML-affected SMB sampled from the mainstem of the Susquehanna River (SUSHM8; PV454363). We recovered a complete genome of an additional novel adomavirus (*Micropterus nigricans adomavirus 1*; PV430023) with a circularized length of 15,989 bp from a HPML lesions affecting an LMB specimen from Lake St. Clair, MI (S2 Fig).

Although the intent of this research was not to evaluate the geospatial distribution of BBS, the external presentation of pathognomonic HPMLs, hallmark of this disease, facilitated observation and collection of samples from geographically disparate regions of the United States. To confirm an association of adomaviruses with HPMLs we screened samples from clinically normal skin and HPMLs for the presence of viral DNA. We detected the viral helicase gene RepE1 in 100% and 95.2% of HPMLs from samples screened for MdA-1 (n=49) and MnA-1 (n=63), respectively (S1 Table). PCR product for RepE1 was never detected in normal skin samples (n=14) from clinically affected fish nor clinically normal fish (n=20). We screened two raised mucoid skin lesions (RMSLs) on SMB skin (S3 Fig), a lesion-type which we have previously ascribed to a different adomavirus, MdA-2 [42]. They were both PCR positive for MdA-2, but negative for MdA-1. Of note, both MdA-1 and MdA-2 were present in metagenomic and metatranscriptomic libraries of RMSLs (SRR10512798 and SRR10540651, respectively) deposited in the Sequence Read Archive (SRA) based on PebbleScout queries and local *in silico* mapping [43]. Albeit, MdA-1 was present orders of magnitude lower than MdA-2 (29x and 57260x coverage respectively). Further, we never detected MdA-1 in LMB nor MnA-1 in SMB.

Relative expression of viral genes in HPMLs

We evaluated the relative expression of viral genes in skin samples from LMB and SMB. The intention was to verify active infection and survey expression patterns of viral genes. Analyses included SMB collected from the Susquehanna River Watershed (PA) in late April 2017 and May 2022, and LMB from Little Hunting and Dogue Creek (VA) in April 2022. Low variability in expression profiles across temporally matched samples (Fig 3A and B) suggested a seasonal synchronicity of the viral lifecycle in naturally infected fish. Notably, expression patterns were similar between MdA-1 and MnA-1 in the different bass species collected during

2022 suggesting similar lifecycle strategies between these viruses. Across samples, the viral helicase gene (RepE1) presumed to be an early expressed gene was among the least abundant viral transcripts suggesting that fish were in late-stage infection.

In contrast, MdA-1 expression profiles from SMB samples collected in 2022 were quantitatively dissimilar from fish collected in 2017 (Fig 3B and C). Although this may highlight annual variation (April 2017 vs May 2022), expression patterns between fish from the same site during the same sampling season were remarkably similar. These differences across years, yet time and site-specific similarities further suggests a coordinated seasonal progression in the differential expression of viral genes.

Localization of viral RNA within HPMLs

In an effort to identify the cell-type(s) infected by these adomaviruses, we developed RNAScope probes specific to the adenain transcripts of MdA-1 and MnA-1. Adenain was targeted given that RNA-seq results from HPMLs sampled in 2017 identified it as the most abundant viral transcript. Given the small dsDNA genome of these viruses, RNAScope probes also effectively targeted viral DNA which was evident in the nucleus of virus positive epithelial cells. In spring-collected samples from LMB and SMB, perinuclear staining was observed in melanocytes that had migrated to the epidermis indicating viral replication in this cell type (Fig 4). A cytoplasmic signal was not observed in melanocytes. Virus positive cells were also observed within the basement membrane in LMB infected with MnA-1 (S4 Fig). Notably, we identified viral transcripts in the cytoplasm of epithelial cells within the epidermis of a fall-collected SMB (S5 Fig). Nuclear staining of viral nucleic acids was evident in these cells as well. In fall-collected SMB, virus negative melanocytes were often observed proximate to virus positive cells in HPMLs. This suggests that the proliferation and infiltration of melanocytes from

the dermis to the epidermis during the fall was part of a host response to viral infection. Positive signal was not observed in clinically normal skin.

Phylogenetically related, but different adomaviruses are associated with HPMLs in largemouth and smallmouth bass

Consistent with other adomaviruses, MdA-1 and MnA-1 encode two cassettes of bidirectionally transcribed genes (Fig 5) [31, 44, 45]. The annotated genomes included core genes associated with adomaviruses including Cah (hypothetical capsid-surface protein with predicted alpha helical [particularly coiled-coil] character), Penton (pentameric single β- jellyroll capsid protein), Macc (hypothetical membrane-active capsid core protein), Hexon (double β-jellyroll major capsid protein that trimerizes to form virion facets), Adenain (papain-like cysteine protease involved in virion maturation), Prim (homolog of archaeal-eukaryotic primase small catalytic subunits), Rep (superfamily 3 ATP-dependent replicative DNA helicase with N-terminal nicking endonuclease-like domain) and SET (Su(var)3-9 Enhancer-of-Zeste and Trithorax homologue). In addition to these core genes, there were predicted open reading frames (ORFs) encoding genes with no clear homologues in GenBank or HHPred searches. These included: Endonoid (Endonuclease like protein), Phogi (remote similarity to phosphoglucose isomerase), Herpeto (remote similarity to Herpeto_peptide), Zifi (Nab2-type zinc finger), Col (predicted collagen-like fold), and Wasp (WASP actin regulatory protein-like). Neologisms were assigned based on HHpred and AlphaFold/DALI best hits or by synteny adopted from previous adomavirus annotation efforts [31]. Predicted protein structures differed across these syntenic ORFs as well as HHpred and DALI predictions, but we retained syntenic naming assignments for simplicity.

Genome alignment of MdA-1 and MnA-1 indicated 68.0% nucleotide identity. Predicted coding sequences (CDS) were similar across the genomes, yet there were a few distinctive differences. Open reading frames encoding homologs of MdA-1 Endonoid and Phogi were not predicted in MnA-1. In this genomic region upstream of Col, another ORF (Zifi) was identified in MnA-1 encoding a predicted Nab2-type zinc finger. The MnA-1 genome also included an overprinted ALTO ORF within RepE1. A possible ALTO-like ORF in MdA-1 is interrupted by a nonsense mutation. Amino acid identity across shared predicted proteins ranged from 41.0 (Colalt) to 92.2% (Hexon; Table 2). In general, there was a notable decrease in protein identity in ORFs upstream of Cah. Predicted proteins in this region shared 63.3% identity or less between the two viruses. This included Col, Colalt and Wasp which we named based on synteny alone. This region also included divergent protein coding regions. Predicted three-dimensional protein structures of these proteins, and results of HHpred and DALI further emphasize the dissimilarity (Fig 6, S6 Fig, S7 Fig, S3 Table, S4 Table). Notably, HHpred and Dali predictions for Wasp from both MdA-1 and MnA-1 suggested similarity to porphyrins and myoglobin (S7 Fig). DALI yielded no results for MnA-1 Col. A predicted retinoblastoma pAB groove interacting motif was identified within RepE1 of both viruses, suggesting potential interactions with host tumor suppressing genes.

Table 2. Pairwise protein identity between predicted proteins of MdA-1 and MnA-1. Proteins are sorted by % identity. ALTO, Endonoid, Herpeto, Phogi and Zifi were not included in pairwise comparisons given that they were unique.

Protein	% Identity
Hexon	92.2
Penton	86.8
Penton+	83.4
Cah	82.5
RepE1	78.9
Prim	76.9
Macc	74.0
Adenain	72.4
Col	63.3
SET	62.0
Wasp	51.7
Alt	49.3
Colalt	41.0

Genetic diversity across bass adomaviruses

Given the recent, concurrent emergence of BBS in disparate watersheds, we compared partial sequences of RepE1 across MdA-1 samples from SMB collected from Michigan, Pennsylvania and Vermont to gain insights into genetic diversity across samples as a preliminary epidemiological survey (S1 Table). Sequences obtained from the same location were always identical across the 699 bp PCR amplicon (Fig 7A, Fig 8A), whereas four base substitutions were noted between sites. All single nucleotide polymorphisms (SNPs) were synonymous transversions; A↔C (1) or C↔G (4). Complete genome alignments of the two MdA-1 isolates

from PA during different years identified only 14 nucleotide differences across the genomes (99.9% identical) and no difference in the RepE1 amplicon region (S7 Fig), suggesting *prima facie* an overall low rate of accepted mutations within populations. Notably, of these SNPs only those within the Col and Wasp ORFs led to protein coding changes (Col; 99.5% and Wasp; 99.4% protein identity).

We compared a similar region of MnA-1 RepE1 from clinically affected LMB housed in live exhibits at Bass Pro Shops (BPS) located in different states across the USA as well as wild-caught fish from MI, VA, and TX. We observed up to 21 nucleotide differences (97.4% identity) across some samples. These were restricted to three samples that likely represent a different subtype of MnA-1 (Fig 7B). Whole-genome reconstructions of MnA-1 from these RepE1 distinctive samples are not available. Across this 805 bp locus, samples from six different locations were identical (Fig 8B). Identified SNPs were represented by both transitions (C↔T [9] and A↔G [5]) and transversions (G↔T [3], A↔C [2] and A↔T [2]). Notably, the nucleotide differences in the most divergent clade only led to two amino acid changes. When sequences from this distinct clade were not considered, we only observed at most two nucleotide differences between samples. Unfortunately, the origin of fish from BPS was not always known, and phylogeographic inferences for MnA-1 in wild fish are limited. Nonetheless, it can be concluded that the MnA-1 does not show the strong geographic structure apparent in MdA-1 based on this sampling.

Phylogenetic placement of novel adomaviruses

Phylogenetic analysis of the replicase genes of the bass adomaviruses and other publicly available adomaviruses placed these viruses in a clade of RepE1 adomaviruses associated with a subgroup of African cichlids (subfamily Pseudocrenilabrinae; Fig 9). In general, the RepE1,

RepLT and CressRep proteins resolved to distinct groups or to a clade represented by family-level taxa. CressRep was restricted to invertebrate hosts (specifically Bivalvia), but adomavirus replicases are not monophyletic. Subclades of RepE1 or RepLT were best predicted by host taxa. Similar phylogenetic placement was observed using other core adomavirus genes. Greatest sequence homology was observed across hexon proteins (Fig 10). Based on sequence similarity across these three proteins, representative adomaviruses from this clade are more similar to those from reptile hosts (leatherback sea turtle; *Dermochelys coriacea*) than fish hosts. Sequence similarity of adenain or hexon was not a predictor of replicase type which supports the proposal of horizontal gene transfer within this consortium of adomaviruses [46]. Although the three adomaviruses with cichlid hosts that resolved to the clade including MdA-1 and MnA-1 share the same genome architecture, similar to these viruses there is considerable variability in the number and putative identity of ORFs upstream of Col (S8 Fig).

Discussion

Adomaviruses are an enigmatic group of viruses with a circular dsDNA genome related to the small DNA tumor viruses [45, 47]. Their name is a chimeric portmanteau derived from the adeno, papilloma and polyomaviruses for which they share protein homology and mixed elements of syntenic genome architecture. At present this group is represented by nearly 60 complete or partial genomes from a host range that includes invertebrates, fishes, and herptiles, but with greatest representation in fishes [31, 48]. They are broadly defined by a circular genome that is 9-20 kilobase pairs (kb) in length that encodes a superfamily 3 helicase, a candidate Penton, and a candidate Cah-class gene [31]. This group of viruses consists of three classes defined by the polyomavirus-like replicase (RepLT), papillomavirus-like replicase (RepE1), or CRESS-like replicase (CressRep). Notably, most of these viral genomes have been mined from

metagenomic projects, and only a few have been identified in clinically diseased fishes and ascribed as the causative pathogen [31, 45, 48-55]. Although the host-microbe relationships of many adomaviruses are unclear, some representatives of this group lead to substantial disease in fishes and are associated with considerable economic losses in commercial aquaculture settings particularly in the case of anguillids [52-54, 56]. At present the adomaviruses are not formally recognized by the International Committee on Taxonomy of Viruses (ICTV), and are indexed as unclassified dsDNA viruses in the NCBI taxonomy database [57].

Our investigation here was a deliberate attempt to clarify the relationship between a putative, novel adomavirus sequence identified in a SMB deep sequencing project and HPMLs in black basses [10]. Initial screening attempts to confirm virus in HPMLs from SMB routinely verified the presence of adomavirus DNA; however, primer sets for this virus always failed to amplify specific product from the same lesion type on LMB. Deep sequencing and *de novo* assembly approaches were required to identify the adomavirus associated with HPMLs in LMB. The adomaviruses herein described from bass exhibiting BBS are members of the RepE1 class of adomaviruses. While the gross clinical signs of BBS are indistinguishable between LMB and SMB, they appear to be the result of different but related viruses that likely co-evolved with their host upon the divergence of these species around six million years ago [1]. These genomes are only 68.0% identical with notable coding differences affecting the number of predicted viral proteins and identity across cognate proteins. Given these differences and despite the same clinical presentation across these two host species, BBS is caused by two different viruses in these distinct hosts and outcome(s) of viral infection may differ.

While we have not attempted to fulfill Koch's postulates, we feel that Rivers' postulates have been satisfied such that (a) the specific adomaviruses have been found to be associated with

the clinical signs of disease with a degree of regularity, and (b) the adomaviruses were demonstrated to occur in clinically affected individuals not as an incidental or accidental finding but as the cause of the disease under investigation [58]. Moreover, the fact that two related but genetically distinct (68.0% identical) adomaviruses are associated with the hallmark clinical signs of BBS provides indubitable evidence that these viruses are indeed causative agents of this seasonal disease.

The emergence of BBS in SMB from geographically separated watersheds in Michigan, Pennsylvania and Vermont prompted us to hypothesize that perhaps there were recent, sequential introductions of this virus. While our data sets are not comprehensive, the viruses are clearly not identical across these watersheds and more informatively they share identical SNPs in the RepE1 loci specific to geographical collection sites suggestive of phylogeographic differences. Given that viruses with dsDNA genomes accumulate mutations more slowly than other virus-types, we anticipate that future analyses with larger datasets may provide further evidence that these viruses have been evolving in geographic isolation for hundreds to thousands of years and are not the result of recent introductions [59-62]. As an example, evolution rates for polyomaviruses are 0.5% per million years ($5x10^{-9}$) and 1.3×10^{-7} spontaneous mutations per base per infection cycle for adenoviruses under minimal selection [62, 63]. That stated, it should be mentioned that SMB were introduced to the Susquehanna River watershed (PA) during the 1870's but are indigenous to the other sampled locations [64]. Due to the frequent movement of LMB across the country, we anticipate more homologous viral genomes, and this is supported by our current dataset. Our sequencing analyses were limited to a small locus within RepE1 which is a conserved viral helicase gene [65]. Insights into phylodynamics may be better achieved by targeting loci between the SET and Cah ORFs where we observe the greatest predicted protein

coding differences between the MdA-1 and MnA-1 genomes, as well as the two MdA-1 genomes [66]. Perhaps this region of the genome is similar to the hypervariable regions of adenoviruses [60]. If indeed new introductions of MdA-1 do not explain the emergence of BBS in these geographically distant watersheds, perhaps changes in thermal profiles at the ecosystem-scale has affected host-microbe balance in a fashion predicted by evolutionary mismatch theory [67].

BBS exhibits strong seasonality and the gross, seasonal manifestation has recently been modelled for SMB in the Susquehana River watershed [24]. Perhaps most unexpected in these data sets is the similarity in expression patterns between individuals at a given collection site considering that these fish were all naturally infected. This coordination suggests that these fish were either exposed to the virus at a similar time, or that environmental triggers such as temperature drive this response. In some regards BBS, resembles the retroviral diseases of walleye (*Stizostedion vitreus*) integument in that it affects adults, is seasonal (fall through spring), and resolves when water temperatures increase [68, 69]. Fish are poikilothermic vertebrates and seasonality of disease is well established and often ascribed to the downregulation of adaptive immune responses in cooler temperature [70-73]. As a result, fishes tend to rely on innate immune responses during these times and perhaps the recruitment of melanocytes is part of this innate immune response [72]. Of particular note, the clinical manifestation of BBS is observed in adults and the observation of clinical signs coincides with the seasonal timing of gonadal recrudescence [24]. This condition is observed in males and females, but it is unknown if there is a sex bias in respect to prevalence or severity. We anticipate that there is a physiological sex steroid background profile that influences this disease presentation. Elevated androgens and estrogens are part of the normal adult physiology during gonadal recrudescence which occurs during the fall through late spring in these temperate basses

depending on latitude [74, 75]. This may explain the anecdotal observation that large healthy-looking fish of high condition factor seem to be disproportionally affected given that these fish typically have higher steroid hormone concentrations. Although HPMLs are not melanomas, they are composed of the same, but non-transformed cell-type for which androgens have been demonstrated to drive melanoma invasiveness [76]. Perhaps a similar steroid-mediated mechanism drives melanocyte migration in BBS.

Based on RNAScope evidence, it appears that the development of the hallmark melanistic blotches shared across the bass species here is likely an orchestrated host response to viral infection, rather than the direct result of melanocyte infection. Epithelial cells in the integument appear to be the primary cell-type infected with virus during the early phase (fall) of grossly observable disease. Proliferation and infiltration of melanocytes into the epidermis is observed at this stage. Melanocytes are clearly permissive to infection evinced by perinuclear staining of this cell type during a later stage of natural infection (spring). Similar to the reports of adomavirus infection in giant guitarfish (*Rhynchobatus djiddensis*) and sand tiger sharks (*Carcharias taurus*), epithelial cells of the epidermis appear to be the initial target cell of infection [45, 55]. Melanization is also associated with lesions in guitarfish and clinical disease appears to be transient [77]. Interestingly, there is some evidence that cichlids, including *Perissodus microlepis*, exhibit HPMLs reminiscent of lesions observed in BBS. If melanization is the result of a host response to viral infection, there must be a stage of this disease when tissues are virus positive prior to the clinical observation of HPMLs.

Although melanocytes are commonly recognized for their photoprotective role to ultraviolet electromagnetic radiation by the melanin they produce, this cell type is also an antigen presenting cell (APC) similar to macrophages and dendritic cells - although they originate from

the neural crest rather than from hematopoietic tissues [78]. While melanocytes are not classified as professional APCs, they do share functional similarly in that they are phagocytic and express the class II major histocompatibility complex upon IFNγ stimulation. They are involved in host defenses via phagocytosis and antigen presentation to T cells, secrete pro- or anti-inflammatory cytokines to regulate immune responses and are an important cell type in innate immunity to multiple pathogen types including viruses [79-83]. Inflammatory mediators have been demonstrated to promote melanogenesis [80]. Evidence supports that the M2 macrophage phenotype associated with post-infection tissue remodeling are responsible for providing an anti-inflammatory cytokine environment that promotes skin pigmentation [84]. Intermediates formed during melanogenesis are have potent antimicrobial properties [85]. Given the clinical interest in melanin and its association with diseases, perhaps BBS may serve as a model for therapeutic research in humans as specific viral proteins are likely associated with the melanistic response [86].

Although BBS is associated with viral infection, it is unclear if it has detrimental health effects. The syndrome has been observed in LMB for nearly 40 years and there have been no clear, negative health effects. During this time frame, if these highly visible markings of hyperpigmented lesions on the surface of bass were associated with substantial mortality events anglers and resource managers would likely have noticed. In the case of SMB, it is noteworthy that the emergence of this clinical presentation was observed after years of chronic mortality events that impacted the population structure [87]. It is also notable that ulcerative skin lesions are often infected with opportunistic bacterial pathogens and evidence suggests that LMB virus leads to similar lesions. However, molecular diagnostics were not available or employed to screen for largemouth bass virus (LMBV) nor these novel adomaviruses in this work during fish

kills [9, 88, 89]. Fish affected in these mortality events were also typically of a size class (young-of-the-year) in which clinical BBS is not observed - this may not be indicative of lack of infection but rather lack of a host response). The seemingly simultaneous emergence of the clinical signs of BBS in SMB during the last 15 years in disparate watersheds prompts the question, "What has changed?". The 22-year data set from Lake St. Clair serendipitously captured the emergence of this condition in a world class fishery. Mortality events similar to those in the Susquehanna River have not been reported in Lake St. Clair nor in Lake Champlain, VT. In the case of Lake St. Clair, fisheries managers had been monitoring fish for six years prior to observing blotchy bass at a prevalence that warranted inclusion on their datasheets. Perhaps the most intriguing observation in this data set is that no blotchy fish were reported prior to 2008. Although this does not suggest that blotchy bass were not present, it likely indicates that something may have changed to an extent that this observation became noteworthy of documentation. Since that time, springtime annual variation in blotchy bass has been reported with an average prevalence of 5.1% and as high as 9.2%. This is similar to the prevalence and annual variation observed in the Susquehanna River basin. One unifying commonality between these three regions is that they tout world-class smallmouth bass fisheries and respectively receive extensive angling pressure [24].

Transmission of bass adomaviruses is a black box. Given the fragility of HPMLs during the spring and viral gene expression data suggesting that this is a late phase of viral infection, it is possible that transmission occurs during spawning which involves physical contact such as contact nips during courtship [90]. During the winter months, these fish also congregate in deeper waters at densities that increase the likelihood of physical contact. Angler handling of infected fish may also pose a mechanism of transmission. Unlike that of terrestrial vertebrates,

the skin of fishes is not keratinized and the outermost layer is a mucosal epithelium resembling that of the gut [91]. If indeed epithelial cells are the initial target cell of adomaviruses, minimal disruption to this mucosal layer may be sufficient to facilitate infection. In this instance, handling fish with BBS is likely a risk factor for transmission.

While simply conjecture, one possible explanation could be that hyperpigmentation during spawning season is advantageous and these adomaviruses are beneficial to the host particularly when turbidity increases due to spring run-off. Although less commonly considered in the context of viruses, examples of viral mutualistic symbioses have been documented [92-95]. Melanism and variation in color patterns influence mate selection in fishes [96]. Melanic side-spotting in poecilid fishes has been well investigated particularly in swordtails (*Xiphophorus spp*.). These side-spotting patterns are of low frequency (<30%), and while genetic factors are associated with this phenotype the selection mechanisms are largely unknown [97]. Adomaviruses have recently been identified in swordtails, but no research has been published that evaluates the outcome of infection or whether there is a non-host genetic association with side-spotting. There may be an unexplored relationship between seasonal side-spotting in some fishes associated with adomaviruses.

Hyperpigmented lesions grossly similar to those in the black basses described here have been reported in other fish species. This observation is sometimes reported in the published literature, but more often is communicated by fisheries managers. We have evidence that adomaviruses are associated with those HPMLs in some instances (unpublished data), suggesting that an adomavirus etiology could be investigated in efforts to identify causative agent for instances when metazoan parasites are ruled out. Given the level of divergence in nucleotide sequence across these viruses, such efforts will inevitably require *de novo* sequencing methods

coupled with virus discovery bioinformatic workflows to identify them if indeed present [98-101].

Although the significance of adomavirus infection in black basses is not clear, these viruses are a substantial problem in eel aquaculture that could be abated with the development of an efficacious vaccine development. Due to the external and macroscopically observable clinical signs of adomavirus infection in black basses, development of an infection model for BBS could be developed to test antigen candidates for adomavirus vaccines. Disease outcomes of infectious microbes are often exacerbated in intensive aquaculture conditions [102]. LMB are increasingly cultured for stocking for recreational purposes as well as a commercial food fish. It is prudent that managers take notice of viral diseases such as this with unknown outcomes under different environmental settings. In the instance of blotchy bass syndrome, fish managers can now inform the angling public of the cause of HPMLs based on scientific findings. Additionally, given the microbial nature of this disease more research can be conducted in the context of a causative agent to support the development of management decisions.

Acknowledgements
This research was funded by the Biological Threats and Invasive Species Research Program of the US Geological Survey, Ecosystems Mission Area. We wish to thank Blayk Michaels of Bass Pro Shops and Cabela's for coordinating sample collection efforts from blotchy bass housed in live exhibits. This research would not have been possible without the in-kind support and sampling assistance by the Michigan Department of Natural Resources, Pennsylvania Fish & Boat Commission, Vermont Fish & Wildlife Department, and the Virginia Department of Inland Game and Fisheries. We wish to thank Meghan Kepler-Shall for providing the image of a clinically affected smallmouth bass and anglers for submitting images to the Texas Parks and Wildlife Department. Any use of trade, firm, or product names is for descriptive purposes only and does not imply endorsement by the U.S. Government. The USDA is an equal opportunity employer. Supporting data are archived in FigShare.

References

1. Kim D, Taylor AT, Near TJ. Phylogenomics and species delimitation of the economically important Black Basses (Micropterus). Scientific reports. 2022;12(1):9113. Epub 20220606. doi: 10.1038/s41598-022-11743-2. PubMed PMID: 35668124; PubMed Central PMCID: PMCPMC9170712.
2. Associates S. Sportfishing in America: A Reliable Economic Force. 2020.
3. Tidwell J, Coyle S, Bright LA. Largemouth bass aquaculture. 2018.
4. Taylor AT, Long JM, Tringali MD, Barthel BL. Conservation of Black Bass Diversity: An Emerging Management Paradigm. Fisheries. 2019;44(1):20-36. doi: https://doi.org/10.1002/fsh.10187.
5. Seguy L, Long JM. Perceived Ecological Threats and Economic Benefits of Non-Native Black Bass in the United States. Fisheries. 2021;46(2):56-65. doi: https://doi.org/10.1002/fsh.10520.
6. Yu P, Chen H, Liu M, Zhong H, Wang X, Wu Y, et al. Current status and application of largemouth bass (Micropterus salmoides) germplasm resources. Reproduction and Breeding. 2024;4(2):73-82. doi: https://doi.org/10.1016/j.repbre.2024.01.004.
7. Li Y, Wagner T, Jiao Y, Lorantas R, Murphy CA. Evaluating spatial and temporal variability in growth and mortality for recreational fisheries with limited catch data. Canadian Journal of Fisheries and Aquatic Sciences. 2017;75(9):1436-52. doi: 10.1139/cjfas-2017-0052.
8. Smith G, Blazer V, Walsh H, Iwanowicz LR, Starliper CE, Sperry A. The Effects of Disease-Related Mortality of Young-of-Year Smallmouth Bass on Population Characteristics in the Susquehanna River Basin, Pennsylvania and Potential Implications to Conservation of Black Bass Diversity. American Fisheries Society Symposium: American Fisheries Society; 2015.
9. Blazer VS, Iwanowicz LR, Starliper CE, Iwanowicz DD, Barbash P, Hedrick JD, et al. Mortality of centrarchid fishes in the Potomac drainage: survey results and overview of potential contributing factors. J Aquat Anim Health. 2010;22(3):190-218. Epub 2011/01/01. doi: 10.1577/H10-002.1. PubMed PMID: 21192549.
10. Blazer VS, Young KT, Smith GD, Sperry AJ, Iwanowicz LR. Hyperpigmented melanistic skin lesions of smallmouth bass Micropterus dolomieu from the Chesapeake Bay watershed. Dis Aquat Organ. 2020;139:199-212. Epub 2020/06/05. doi: 10.3354/dao03480. PubMed PMID: 32495746.
11. Blazer V, Mazik PM, Iwanowicz LR, Braham R, Hahn C, Walsh HL, Sperry A. Monitoring of wild fish health at selected sites in the Great Lakes Basin: methods and preliminary results. Report. Reston, VA: 2014 2014-1027.
12. Carlson DM. Unusual pigmentation on largemouth bass. Proceedings of the 45th Annual Northeast Fish and Wildlife Conference. 1989.
13. Blazer VS, Mazik P, Iwanowicz LR, Braham RP, Hahn CM, Walsh HL, Sperry A. Monitoring of wild fish health at selected sites in the Great Lakes Basin—Methods and preliminary results. U.S. Geological Survey Open-File Report. 2014 2014. Report No.
14. Sweet M, Kirkham N, Bendall M, Currey L, Bythell J, Heupel M. Evidence of melanoma in wild marine fish populations. PloS one. 2012;7(8):e41989. Epub 2012/08/08. doi: 10.1371/journal.pone.0041989. PubMed PMID: 22870273; PubMed Central PMCID: PMCPMC3411568.
15. Noguera PA, Feist SW, Bateman KS, Lang T, Grutjen F, Bruno DW. Hyperpigmentation in North Sea dab Limanda limanda. II. Macroscopic and microscopic characteristics and pathogen screening. Dis Aquat Organ. 2013;103(1):25-34. Epub 2013/03/14. doi: 10.3354/dao02553. PubMed PMID: 23482382.
16. Sakamoto K, White MR. Dermal melanoma with schwannoma-like differentiation in a brown bullhead catfish (Ictalurus nebulosus). Journal of veterinary diagnostic investigation : official publication of the American Association of Veterinary Laboratory Diagnosticians, Inc. 2002;14(3):247-50. Epub 2002/05/30. doi: 10.1177/104063870201400311. PubMed PMID: 12033683.

17. Ramos P, Victor P, Branco S. Spontaneous melanotic lesions in axillary seabream, Pagellus acarne (Risso). Journal of fish diseases. 2013;36(9):769-77. Epub 2013/02/07. doi: 10.1111/jfd.12031. PubMed PMID: 23383748.
18. Work TM, Aeby GS. Skin pathology in Hawaiian goldring surgeonfish, Ctenochaetus strigosus (Bennett). Journal of fish diseases. 2014;37(4):357-62. Epub 20130426. doi: 10.1111/jfd.12112. PubMed PMID: 23617760.
19. Okihiro MS, Whipple JA, Groff JM, Hinton DE. Chromatophoromas and chromatophore hyperplasia in Pacific rockfish (Sebastes spp.). Cancer Res. 1993;53(8):1761-9. Epub 1993/04/15. PubMed PMID: 8467494.
20. Kohl ZF, Calhoun DM, Elmer F, Peachey RBJ, Leslie KL, Tkach V, et al. Black-spot syndrome in Caribbean fishes linked to trematode parasite infection (Scaphanocephalus expansus). Coral Reefs. 2019;38(5):917-30. doi: 10.1007/s00338-019-01819-3.
21. Duflot M, Cresson P, Julien M, Chartier L, Bourgau O, Palomba M, et al. Black spot diseases in seven commercial fish species from the English Channel and the North Sea: infestation levels, identification and population genetics of Cryptocotyle spp. Parasite. 2023;30:28. Epub 20230706. doi: 10.1051/parasite/2023028. PubMed PMID: 37417833; PubMed Central PMCID: PMCPMC10327545.
22. Williams MO. The Neascus (Posthodiplostomulum) Stage of Posthodiplostomutn nanum Dubois and an Experimental Determination of Part of the Life Cycle. Journal of Helminthology. 1967;41(2-3):269-76. Epub 2009/06/05. doi: 10.1017/S0022149X00021659.
23. Kinae N, Yamashita M, Tomita I, Kimura I, Ishida H, Kumai H, Nakamura G. A possible correlation between environmental chemicals and pigment cell neoplasia in fish. Science of The Total Environment. 1990;94(1):143-53. doi: https://doi.org/10.1016/0048-9697(90)90369-6.
24. Schall Megan K, Smith Geoffrey D, Blazer Vicki S, Walsh Heather L, Wagner T. Factors Influencing the Prevalence of Hyperpigmented Melanistic Lesions in Smallmouth Bass Micropterus dolomieu in the Susquehanna River Basin, Pennsylvania. Journal of fish diseases. 2024;n/a(n/a):e14033. doi: https://doi.org/10.1111/jfd.14033.
25. Blazer VS, Walsh HL, Smith CR, Gordon SE, Keplinger BJ, Wertz TA. Tissue distribution and temporal and spatial assessment of per- and polyfluoroalkyl substances (PFAS) in smallmouth bass (Micropterus dolomieu) in the mid-Atlantic United States. Environmental Science and Pollution Research. 2024;31(49):59302-19. doi: 10.1007/s11356-024-35097-6.
26. Koressaar T, Remm M. Enhancements and modifications of primer design program Primer3. Bioinformatics (Oxford, England). 2007;23(10):1289-91. Epub 20070322. doi: 10.1093/bioinformatics/btm091. PubMed PMID: 17379693.
27. Zimmermann L, Stephens A, Nam SZ, Rau D, Kübler J, Lozajic M, et al. A Completely Reimplemented MPI Bioinformatics Toolkit with a New HHpred Server at its Core. J Mol Biol. 2018;430(15):2237-43. Epub 20171216. doi: 10.1016/j.jmb.2017.12.007. PubMed PMID: 29258817.
28. Baek M, DiMaio F, Anishchenko I, Dauparas J, Ovchinnikov S, Lee GR, et al. Accurate prediction of protein structures and interactions using a three-track neural network. Science. 2021;373(6557):871-6. Epub 20210715. doi: 10.1126/science.abj8754. PubMed PMID: 34282049; PubMed Central PMCID: PMCPMC7612213.
29. Holm L, Laiho A, Törönen P, Salgado M. DALI shines a light on remote homologs: One hundred discoveries. Protein Sci. 2023;32(1):e4519. doi: 10.1002/pro.4519. PubMed PMID: 36419248; PubMed Central PMCID: PMCPMC9793968.
30. Jumper J, Evans R, Pritzel A, Green T, Figurnov M, Ronneberger O, et al. Highly accurate protein structure prediction with AlphaFold. Nature. 2021;596(7873):583-9. doi: 10.1038/s41586-021-03819-2.
31. Buck CB, Welch N, Belford AK, Varsani A, Pastrana DV, Tisza MJ, Starrett GJ. Widespread Horizontal Gene Transfer Among Animal Viruses. bioRxiv. 2024. Epub 20240326. doi: 10.1101/2024.03.25.586562. PubMed PMID: 38712252; PubMed Central PMCID: PMCPMC11071296.

32. Nomburg J, Doherty EE, Price N, Bellieny-Rabelo D, Zhu YK, Doudna JA. Birth of protein folds and functions in the virome. Nature. 2024. doi: 10.1038/s41586-024-07809-y.
33. Edgar RC. MUSCLE: multiple sequence alignment with high accuracy and high throughput. Nucleic acids research. 2004;32(5):1792-7. Epub 2004/03/23. doi: 10.1093/nar/gkh340. PubMed PMID: 15034147; PubMed Central PMCID: PMC390337.
34. Blazer VS, Iwanowicz DD, Walsh HL, Sperry AJ, Iwanowicz LR, Alvarez DA, et al. Reproductive health indicators of fishes from Pennsylvania watersheds: association with chemicals of emerging concern. Environmental monitoring and assessment. 2014;186(10):6471-91. Epub 2014/06/18. doi: 10.1007/s10661-014-3868-5. PubMed PMID: 24934131; PubMed Central PMCID: PMC4149881.
35. Patro R, Duggal G, Love MI, Irizarry RA, Kingsford C. Salmon provides fast and bias-aware quantification of transcript expression. Nature methods. 2017;14(4):417-9. doi: 10.1038/nmeth.4197.
36. Shen W, Le S, Li Y, Hu F. SeqKit: A Cross-Platform and Ultrafast Toolkit for FASTA/Q File Manipulation. PloS one. 2016;11(10):e0163962. Epub 20161005. doi: 10.1371/journal.pone.0163962. PubMed PMID: 27706213; PubMed Central PMCID: PMCPMC5051824.
37. Soneson C, Love MI, Robinson MD. Differential analyses for RNA-seq: transcript-level estimates improve gene-level inferences. F1000Res. 2015;4:1521. Epub 20151230. doi: 10.12688/f1000research.7563.2. PubMed PMID: 26925227; PubMed Central PMCID: PMCPMC4712774.
38. Love MI, Huber W, Anders S. Moderated estimation of fold change and dispersion for RNA-seq data with DESeq2. Genome Biology. 2014;15(12):550. doi: 10.1186/s13059-014-0550-8.
39. Trifinopoulos J, Nguyen L-T, von Haeseler A, Minh BQ. W-IQ-TREE: a fast online phylogenetic tool for maximum likelihood analysis. Nucleic acids research. 2016;44(W1):W232-W5. doi: 10.1093/nar/gkw256.
40. Letunic I, Bork P. Interactive Tree Of Life (iTOL) v4: recent updates and new developments. Nucleic acids research. 2019;47(W1):W256-W9.
41. Muhire BM, Varsani A, Martin DP. SDT: A Virus Classification Tool Based on Pairwise Sequence Alignment and Identity Calculation. PloS one. 2014;9(9):e108277. doi: 10.1371/journal.pone.0108277.
42. Iwanowicz LR, Young KT, Adams CR, Blazer VS, Smith GD, Cornman RS. Draft Genome Sequence of an Adomavirus Associated with Raised Mucoid Skin Lesions on Smallmouth Bass (Micropterus dolomieu). Microbiol Resour Announc. 2020;9(14). Epub 2020/04/04. doi: 10.1128/mra.01479-19. PubMed PMID: 32241864; PubMed Central PMCID: PMCPMC7118190.
43. Shiryev SA, Agarwala R. Indexing and searching petabase-scale nucleotide resources. Nature methods. 2024;21(6):994-1002. doi: 10.1038/s41592-024-02280-z.
44. Welch NL, Tisza MJ, Starrett GJ, Belford AK, Pastrana DV, Pang Y-YS, et al. Identification of Adomavirus Virion Proteins. bioRxiv. 2020:341131. doi: 10.1101/341131.
45. Dill JA, Camus AC, Leary JH, Ng TFF. Microscopic and Molecular Evidence of the First Elasmobranch Adomavirus, the Cause of Skin Disease in a Giant Guitarfish, Rhynchobatus djiddensis. mBio. 2018;9(3):e00185-18. doi: 10.1128/mBio.00185-18.
46. Buck CB, Welch N, Belford AK, Varsani A, Pastrana DV, Tisza MJ, Starrett GJ. Widespread Horizontal Gene Transfer Among Animal Viruses. eLife Sciences Publications, Ltd; 2024.
47. Welch NL, Yutin N, Dill JA, Camus AC, Pang Y-YS, Schiller JT, et al. Adomaviruses: an emerging virus family provides insights into DNA virus evolution. bioRxiv. 2018:341131. doi: 10.1101/341131.
48. Harding EF, Russo AG, Yan GJH, Mercer LK, White PA. Revealing the uncharacterised diversity of amphibian and reptile viruses. ISME Communications. 2022;2(1):95. doi: 10.1038/s43705-022-00180-x.
49. Costa Vincenzo A, Holmes Edward C. Diversity, evolution, and emergence of fish viruses. Journal of Virology. 2024;98(6):e00118-24. doi: 10.1128/jvi.00118-24.

50. Waller SJ, Egan E, Crow S, Charsley A, Lokman PM, Williams EK, et al. Host and geography impact virus diversity in New Zealand's longfin and shortfin eels. Archives of virology. 2024;169(4):85. doi: 10.1007/s00705-024-06019-1.
51. Grimwood RM, Fortune-Kelly G, Holmes EC, Ingram T, Geoghegan JL. Host specificity shapes fish viromes across lakes on an isolated remote island. Virology. 2023;587:109884. doi: https://doi.org/10.1016/j.virol.2023.109884.
52. Pao HY, Wu CY, Wen CM. Persistent development of adomavirus and aquareovirus in a novel cell line from marbled eel with petechial skin haemorrhage. Journal of fish diseases. 2019;42(3):345-55. Epub 2019/01/12. doi: 10.1111/jfd.12939. PubMed PMID: 30632177.
53. Mizutani T, Sayama Y, Nakanishi A, Ochiai H, Sakai K, Wakabayashi K, et al. Novel DNA virus isolated from samples showing endothelial cell necrosis in the Japanese eel, Anguilla japonica. Virology. 2011;412(1):179-87. doi: 10.1016/j.virol.2010.12.057.
54. Chang PH. Chapter 13 - Japanese eel endothelial cell-infecting virus. In: Kibenge FSB, Baldisserotto B, Chong RS-M, editors. Aquaculture Pathophysiology: Academic Press; 2022. p. 185-8.
55. Powell AL, Camus AC, Leary JH, Miller SN, Bell CM, Ng TFF. Novel adomavirus associated with proliferative skin lesions affecting the dermal denticles of a sand tiger shark (Carcharias taurus). Front Vet Sci. 2024;11:1470052. Epub 20241002. doi: 10.3389/fvets.2024.1470052. PubMed PMID: 39415956; PubMed Central PMCID: PMCPMC11480009.
56. Yang J-X, Chen X, Li Y-Y, Song T-Y, Ge J-Q. Isolation of a novel adomavirus from cultured American eels, Anguilla rostrata, with haemorrhagic gill necrosis disease. Journal of fish diseases. 2021;44(11):1811-8. doi: https://doi.org/10.1111/jfd.13500.
57. Walker PJ, Siddell SG, Lefkowitz EJ, Mushegian AR, Adriaenssens EM, Alfenas-Zerbini P, et al. Recent changes to virus taxonomy ratified by the International Committee on Taxonomy of Viruses (2022). Archives of virology. 2022;167(11):2429-40. doi: 10.1007/s00705-022-05516-5.
58. Rivers Thomas M. Viruses and Koch's Postulates. Journal of Bacteriology. 1937;33(1):1-12. doi: 10.1128/jb.33.1.1-12.1937.
59. Szpara ML, Van Doorslaer K. Mechanisms of DNA Virus Evolution. Encyclopedia of Virology. 2021:71-8. Epub 20210301. doi: 10.1016/b978-0-12-809633-8.20993-x. PubMed Central PMCID: PMCPMC7173537.
60. Robinson CM, Singh G, Lee JY, Dehghan S, Rajaiya J, Liu EB, et al. Molecular evolution of human adenoviruses. Scientific reports. 2013;3(1):1812. doi: 10.1038/srep01812.
61. Van Doorslaer K. Evolution of the Papillomaviridae. Virology. 2013;445(1):11-20. doi: https://doi.org/10.1016/j.virol.2013.05.012.
62. Buck CB, Van Doorslaer K, Peretti A, Geoghegan EM, Tisza MJ, An P, et al. The Ancient Evolutionary History of Polyomaviruses. PLoS Pathogens. 2016;12(4):e1005574. doi: 10.1371/journal.ppat.1005574. PubMed PMID: PMC4836724.
63. Risso-Ballester J, Cuevas JM, Sanjuán R. Genome-Wide Estimation of the Spontaneous Mutation Rate of Human Adenovirus 5 by High-Fidelity Deep Sequencing. PLoS Pathog. 2016;12(11):e1006013. Epub 20161108. doi: 10.1371/journal.ppat.1006013. PubMed PMID: 27824949; PubMed Central PMCID: PMCPMC5100877.
64. Schall MK, Bartron ML, Wertz T, Niles JM, Shaw CH, Blazer VS, Wagner T. Evaluation of Genetic Population Structure of Smallmouth Bass in the Susquehanna River Basin, Pennsylvania. N Am J Fish Manage. 2017;37(4):850-61. doi: 10.1080/02755947.2017.1327902.
65. Bergvall M, Melendy T, Archambault J. The E1 proteins. Virology. 2013;445(1):35-56. doi: https://doi.org/10.1016/j.virol.2013.07.020.
66. Featherstone LA, Zhang JM, Vaughan TG, Duchene S. Epidemiological inference from pathogen genomes: A review of phylodynamic models and applications. Virus Evolution. 2022;8(1):veac045. doi: 10.1093/ve/veac045.

67. Pollack L, Munson A, Savoca MS, Trimmer PC, Ehlman SM, Gil MA, Sih A. Enhancing the ecological realism of evolutionary mismatch theory. Trends in Ecology & Evolution. 2022;37(3):233-45. doi: https://doi.org/10.1016/j.tree.2021.10.011.
68. Getchell RG, Wooster GA, Bowser PR. Temperature-Associated Regression of Walleye Dermal Sarcoma Tumors. Journal of Aquatic Animal Health. 2000;12(3):189-95. doi: https://doi.org/10.1577/1548-8667(2000)012<0189:TAROWD>2.0.CO;2.
69. Getchell RG, Wooster GA, Rudstam LG, Van DeValk AJ, Brooking TE, Bowser PR. Prevalence of Walleye Discrete Epidermal Hyperplasia by Age-Class in Walleyes from Oneida Lake, New York. Journal of Aquatic Animal Health. 2004;16(1):23-8. doi: https://doi.org/10.1577/H03-076.1.
70. Abram QH, Dixon B, Katzenback BA. Impacts of Low Temperature on the Teleost Immune System. Biology [Internet]. 2017; 6(4). Available from: https://mdpi-res.com/d_attachment/biology/biology-06-00039/article_deploy/biology-06-00039.pdf?version=1511339243.
71. Franke A, Beemelmanns A, Miest JJ. Are fish immunocompetent enough to face climate change? Biology Letters. 2024;20.
72. Scharsack JP, Franke F. Temperature effects on teleost immunity in the light of climate change. Journal of Fish Biology. 2022;101(4):780-96. doi: https://doi.org/10.1111/jfb.15163.
73. Bowden TJ, Thompson KD, Morgan AL, Gratacap RM, Nikoskelainen S. Seasonal variation and the immune response: a fish perspective. Fish & shellfish immunology. 2007;22(6):695-706. Epub 2006/11/23. doi: 10.1016/j.fsi.2006.08.016. PubMed PMID: 17116408.
74. Gross TS, Wieser CM, Sepulveda MS, Wiebe JJ, Schoeb TR, Denslow ND. Characterization of annual reproductive cycles for pond-reared Florida largemouth bass Micropterus salmoides floridanus. American Fisheries Society Symposium. 2002;2002(31):205-12.
75. Iwanowicz LR, Blazer VS, Hitt NP, McCormick SD, DeVault DS, Ottinger CA. Histologic, immunologic and endocrine biomarkers indicate contaminant effects in fishes of the Ashtabula River. Ecotoxicology. 2012;21(1):165-82. Epub 2011/09/02. doi: 10.1007/s10646-011-0776-0. PubMed PMID: 21882039.
76. Liu Q, Adhikari E, Lester DK, Fang B, Johnson JO, Tian Y, et al. Androgen drives melanoma invasiveness and metastatic spread by inducing tumorigenic fucosylation. Nature Communications. 2024;15(1):1148. doi: 10.1038/s41467-024-45324-w.
77. Young K, Seiler S, Yamashita C, Davis S. Surface area of 'blotchy bass' spots change over time in smallmouth bass (Micropterus dolomieu Lacepède, 1802). Keystone J Undergrad Res. 2019;6:1-6.
78. Speeckaert R, Belpaire A, Speeckaert M, van Geel N. The delicate relation between melanocytes and skin immunity: A game of hide and seek. Pigment Cell Melanoma Res. 2022;35(4):392-407. Epub 20220407. doi: 10.1111/pcmr.13037. PubMed PMID: 35298085.
79. Koike S, Yamasaki K. Melanogenesis Connection with Innate Immunity and Toll-Like Receptors. Int J Mol Sci. 2020;21(24). Epub 2020/12/30. doi: 10.3390/ijms21249769. PubMed PMID: 33371432; PubMed Central PMCID: PMCPMC7767451.
80. Fu C, Chen J, Lu J, Yi L, Tong X, Kang L, et al. Roles of inflammation factors in melanogenesis (Review). Mol Med Rep. 2020;21(3):1421-30. Epub 20200117. doi: 10.3892/mmr.2020.10950. PubMed PMID: 32016458; PubMed Central PMCID: PMCPMC7002987.
81. Tam I, Dzierżęga-Lęcznar A, Stępień K. Differential expression of inflammatory cytokines and chemokines in lipopolysaccharide-stimulated melanocytes from lightly and darkly pigmented skin. Exp Dermatol. 2019;28(5):551-60. Epub 20190319. doi: 10.1111/exd.13908. PubMed PMID: 30801846.
82. Zachariae COC, Thestrup-Pedersen K, Matsushima K. Expression and Secretion of Leukocyte Chemotactic Cytokines by Normal Human Melanocytes and Melanoma Cells. Journal of Investigative Dermatology. 1991;97(3):593-9. doi: https://doi.org/10.1111/1523-1747.ep12481934.

83. Swope VB, Krug KA, Nordlund JJ, Abdel-Malek ZA, Sramkoski RM, Babcock GF. Synthesis of Interleukin-1α and β by Normal Human Melanocytes. Journal of Investigative Dermatology. 1994;102(5):749-53. doi: https://doi.org/10.1111/1523-1747.ep12376970.
84. Han H, Kim Y, Mo H, Choi SH, Lee K, Rim YA, Ju JH. Preferential stimulation of melanocytes by M2 macrophages to produce melanin through vascular endothelial growth factor. Scientific reports. 2022;12(1):6416. doi: 10.1038/s41598-022-08163-7.
85. Bjørgen H, Koppang EO. The melano-macrophage: The black leukocyte of fish immunity. Fish & shellfish immunology. 2024;148:109523. doi: https://doi.org/10.1016/j.fsi.2024.109523.
86. Berg SZ, Berg J. Melanin: a unifying theory of disease as exemplified by Parkinson's, Alzheimer's, and Lewy body dementia. Front Immunol. 2023;14:1228530. Epub 20230929. doi: 10.3389/fimmu.2023.1228530. PubMed PMID: 37841274; PubMed Central PMCID: PMCPMC10570809.
87. Schall MK, Smith GD, Blazer VS, Walsh HL, Li Y, Wagner T. A Fishery after the Decline: The Susquehanna River Smallmouth Bass Story. Fisheries. 2020;45(11):576-84. doi: https://doi.org/10.1002/fsh.10491.
88. Boonthai T, Loch TP, Yamashita CJ, Smith GD, Winters AD, Kiupel M, et al. Laboratory investigation into the role of largemouth bass virus (Ranavirus, Iridoviridae) in smallmouth bass mortality events in Pennsylvania rivers. BMC Veterinary Research. 2018;14(1):62. doi: 10.1186/s12917-018-1371-x.
89. Starliper C, Blazer V, Iwanowicz L, Walsh H. Microbial isolates in diseased fishes, primarily smallmouth bass (Micropterus dolomieu), within the Chesapeake Bay drainage in 2009-2011. 2013.
90. Ridgway MS, Goff GP, Miles HAK. Courtship and Spawning Behavior in Smallmouth Bass (Micropterus dolomieui). The American Midland Naturalist. 1989;122(2):209-13. doi: 10.2307/2425905.
91. Xu Z, Parra D, Gómez D, Salinas I, Zhang Y-A, von Gersdorff Jørgensen L, et al. Teleost skin, an ancient mucosal surface that elicits gut-like immune responses. Proceedings of the National Academy of Sciences. 2013;110(32):13097-102. doi: 10.1073/pnas.1304319110.
92. Roossinck MJ. The good viruses: viral mutualistic symbioses. Nature Reviews Microbiology. 2011;9(2):99-108. doi: 10.1038/nrmicro2491.
93. Roossinck MJ, Bazán ER. Symbiosis: Viruses as Intimate Partners. Annual Review of Virology. 2017;4(Volume 4, 2017):123-39. doi: https://doi.org/10.1146/annurev-virology-110615-042323.
94. Jagdale SS, Joshi RS. Enemies with benefits: mutualistic interactions of viruses with lower eukaryotes. Archives of virology. 2018;163(4):821-30. doi: 10.1007/s00705-017-3686-5.
95. Coffman Kelsey A, Harrell Taylor C, Burke Gaelen R. A Mutualistic Poxvirus Exhibits Convergent Evolution with Other Heritable Viruses in Parasitoid Wasps. Journal of Virology. 2020;94(8):10.1128/jvi.02059-19. doi: 10.1128/jvi.02059-19.
96. Culumber ZW, Bautista-Hernández CE, Monks S, Arias-Rodriguez L, Tobler M. Variation in Melanism and Female Preference in Proximate but Ecologically Distinct Environments. Ethology. 2014;120(11):1090-100. doi: https://doi.org/10.1111/eth.12282.
97. Zerulla TC, Stoddard PK. The Biology of Polymorphic Melanic Side-Spotting Patterns in Poeciliid Fishes. Frontiers in Ecology and Evolution. 2021;8. doi: 10.3389/fevo.2020.608289.
98. Peng C, Shang J, Guan J, Wang D, Sun Y. ViraLM: empowering virus discovery through the genome foundation model. Bioinformatics (Oxford, England). 2024;40(12):btae704. doi: 10.1093/bioinformatics/btae704.
99. Tisza MJ, Belford AK, Domínguez-Huerta G, Bolduc B, Buck CB. Cenote-Taker 2 democratizes virus discovery and sequence annotation. Virus Evol. 2021;7(1):veaa100. Epub 2021/01/29. doi: 10.1093/ve/veaa100. PubMed PMID: 33505708; PubMed Central PMCID: PMCPMC7816666.
100. Dong Y, Chen WH, Zhao XM. VirRep: a hybrid language representation learning framework for identifying viruses from human gut metagenomes. Genome Biol. 2024;25(1):177. Epub 20240704. doi: 10.1186/s13059-024-03320-9. PubMed PMID: 38965579; PubMed Central PMCID: PMCPMC11229495.

101. Rangel-Pineros G, Almeida A, Beracochea M, Sakharova E, Marz M, Reyes Muñoz A, et al. VIRify: An integrated detection, annotation and taxonomic classification pipeline using virus-specific protein profile hidden Markov models. PLoS Comput Biol. 2023;19(8):e1011422. Epub 20230828. doi: 10.1371/journal.pcbi.1011422. PubMed PMID: 37639475; PubMed Central PMCID: PMCPMC10491390.
102. Meyer FP. Aquaculture disease and health management. J Anim Sci. 1991;69(10):4201-8. doi: 10.2527/1991.69104201x. PubMed PMID: 1778836.

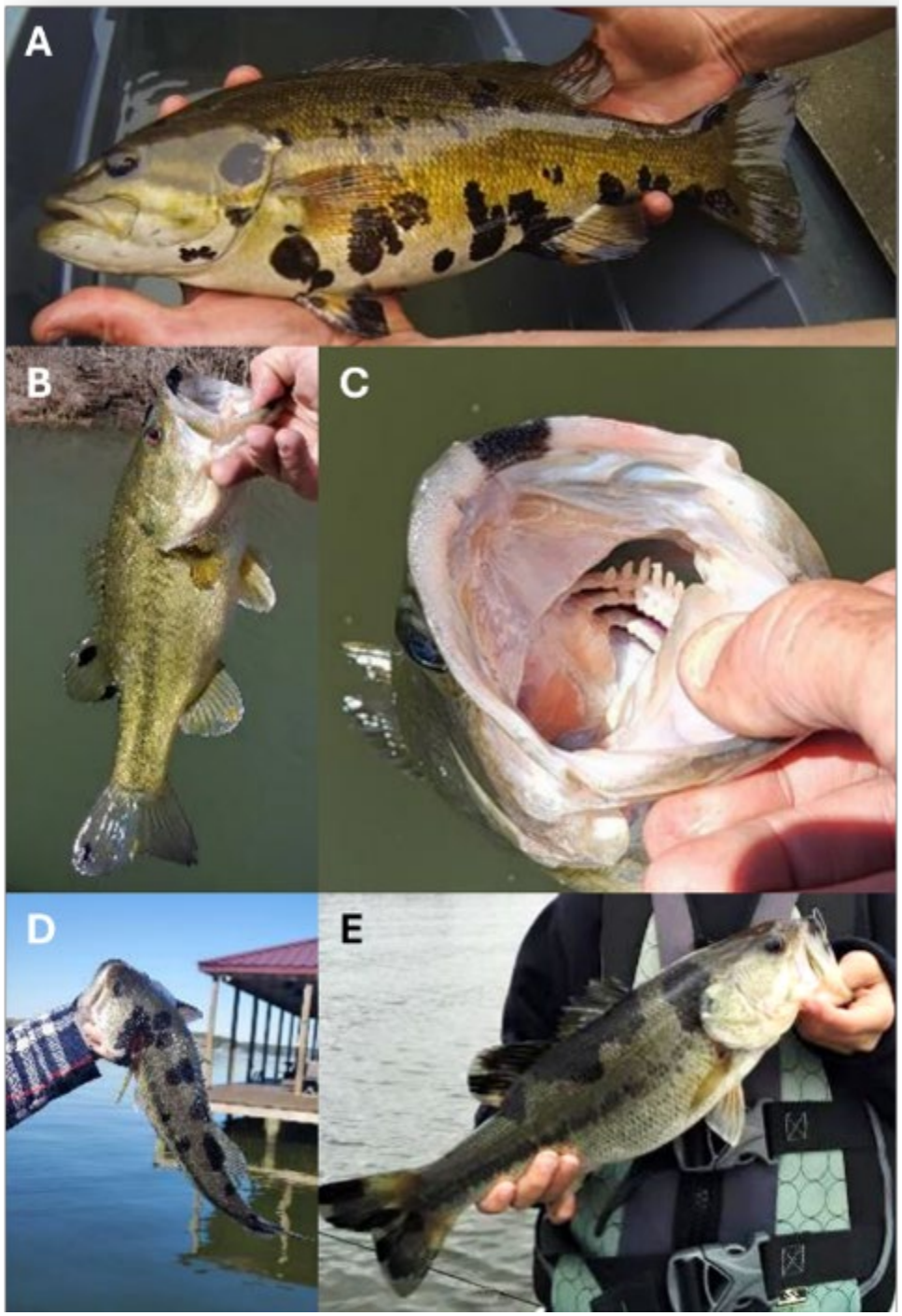

Fig 1. Gross presentation of blotchy bass syndrome in smallmouth and largemouth bass. Hyperpigmented lesions (HPMLs) on the lateral surface of a smallmouth bass (A), HPMLs on the dorsal and caudal fins of a largemouth bass (B), HPML along the premaxilla (C), HMPLs along the dorsolateral surface of a largemouth bass (D), and HPMLs coalescing into a significant area of hyperpigmentation (E).

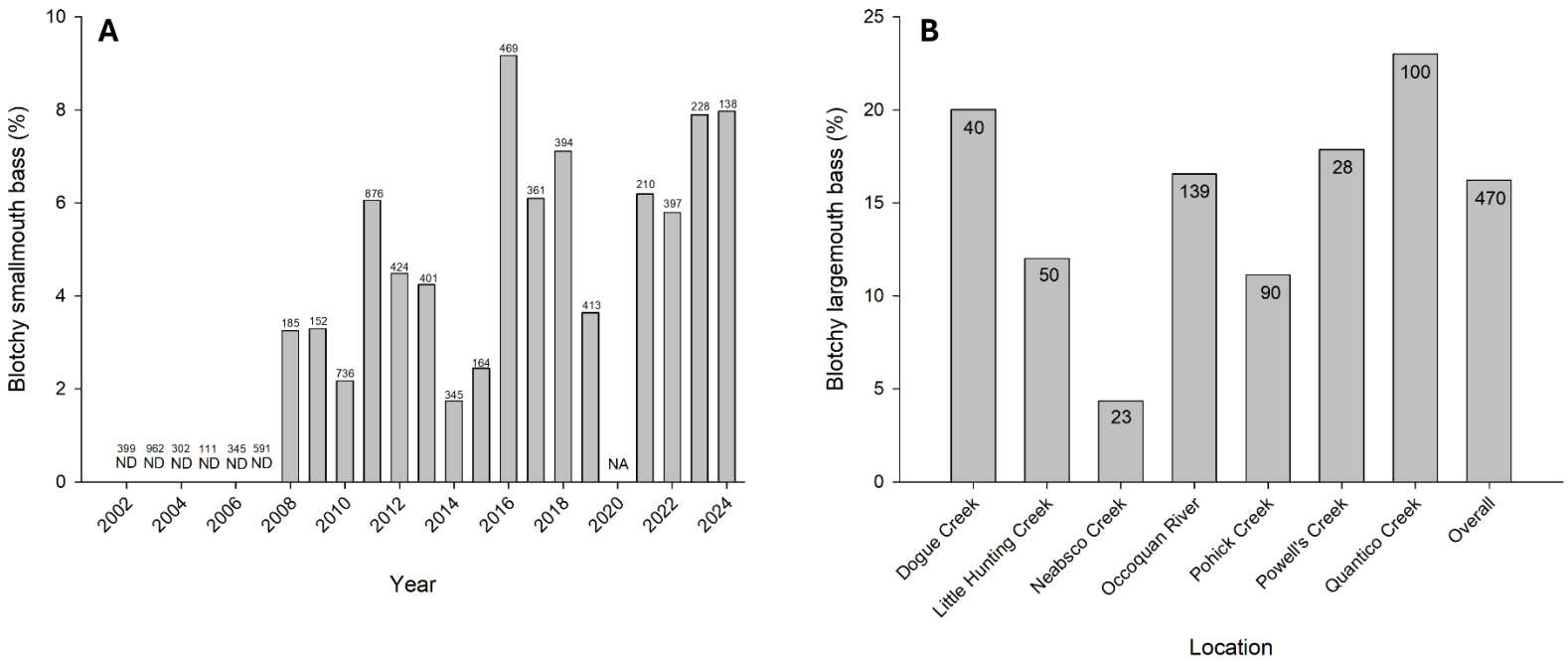

Fig 2. Prevalence of blotchy bass in different geographic locations. (A) Smallmouth bass were samples from Lake St Clair, Minnesota and (B) largemouth bass were sampled from tributaries of the Potomac River in Virginia. Sample size is indicated for each collection. ND indicates not detected, NA indicates data not collected.

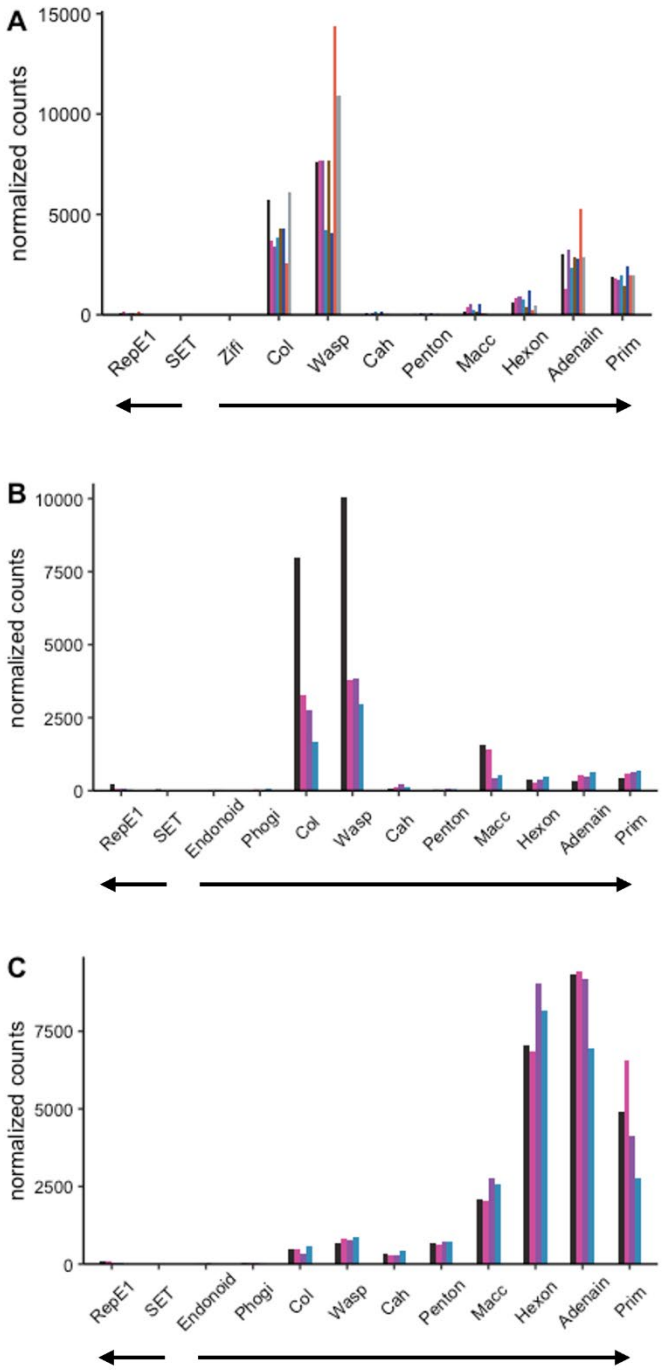

Fig 3. Expression of viral genes in hyperpigmented lesions in large and smallmouth bass. Viral transcript expression was detected in all swabs collected from areas presenting hyperpigmented lesions. Viral transcripts were not detected in swabs from skin regions without hyperpigmentation or in clinical normal fish. (A) MnA-1 in largemouth bass from VA sampled in 2022 (B) MnA-1 from smallmouth bass sampled in PA during 2022 (C) MdA-1 from smallmouth bass sampled in PA during 2017. Genes are arranged in genomic order of open reading frames. Bar colors within each panel indicate transcripts for specific individual fish. Block arrows indicate coding genomic strand.

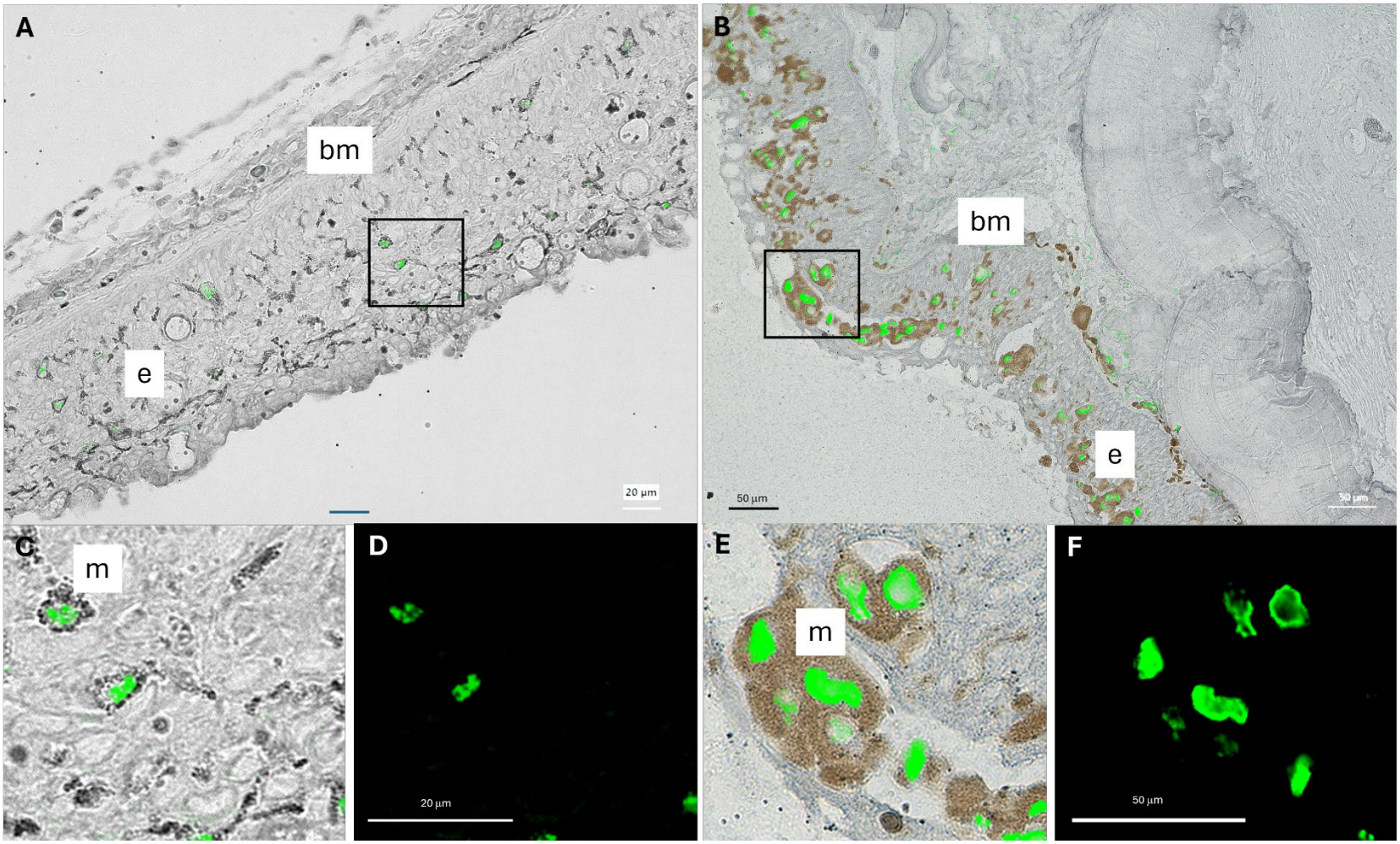

Fig 4. Composite images of histological sections of hyperpigmented lesions on large (A) and smallmouth bass (B). Images represent an overlay of RNAScope probes targeting the adenain sequence of these bass adomaviruses (green) and a brightfield image depicting melanocytes within the integument. Insets (C; overlay) and (D; darkfield); (E; overlay) and (F; darkfield) provide a high magnification view of nuclear staining within melanocytes located in the indicated regions. The epidermis (e), basement membrane (bm) and melanocytes (m) of the integument are indicated.

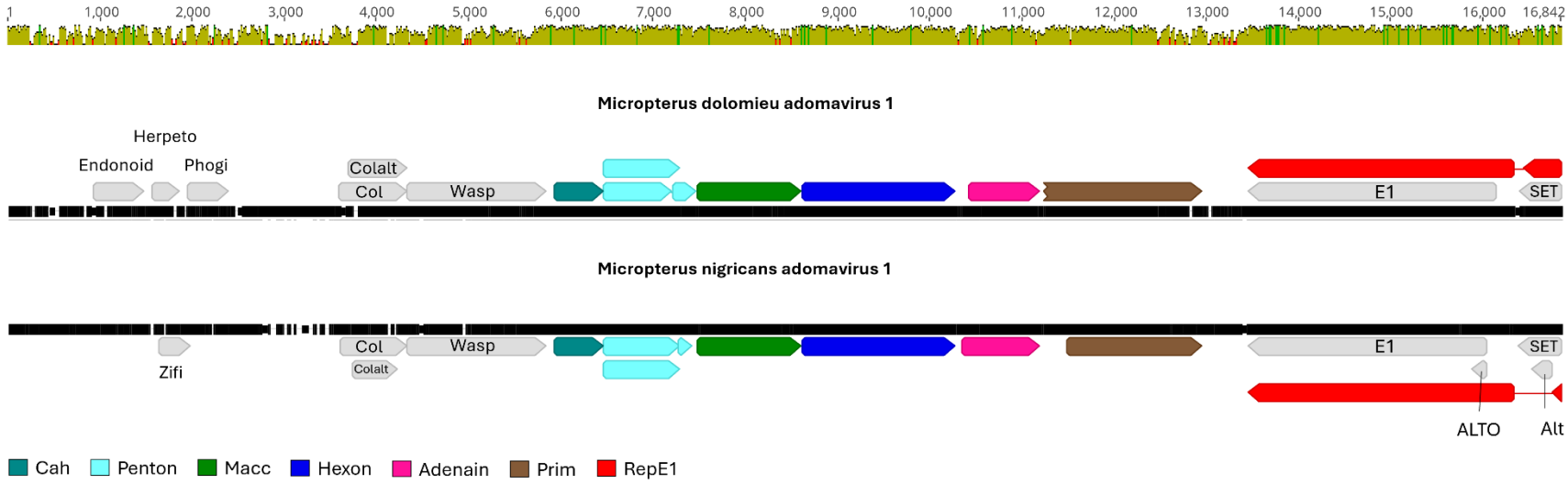

Fig 5. Genome alignment of the smallmouth bass adomavirus 1 (MdA-1) and largemouth bass adomavirus 1 (MnA-1). Core adomavirus open reading frames are colored in non-gray. Identity graph depicts similarity/dissimilarity between the genomes (sliding window = 1).

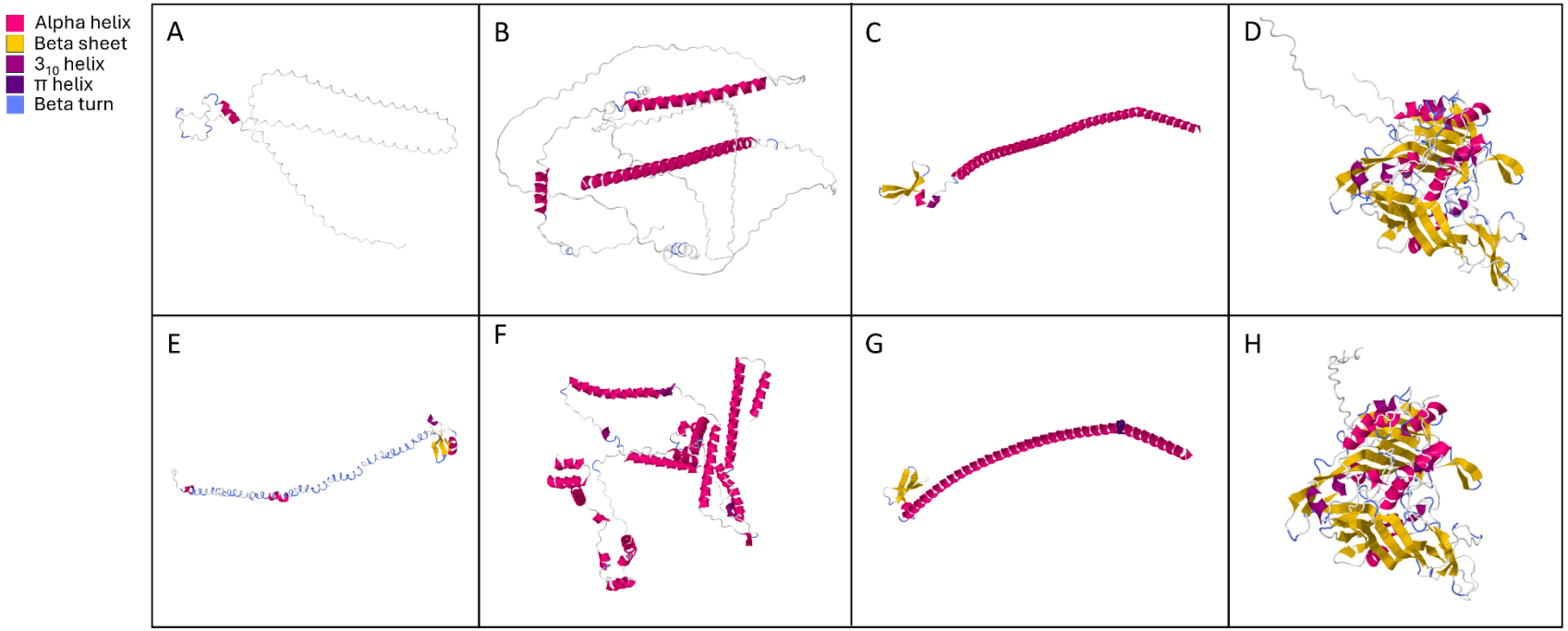

Fig 6. Predicted protein structures of Col (A, E), Wasp (B, F), Cah C, G) and Hexon (D, H) of MdA-1 and MnA-1, respectively. The predicted structures differ markedly between the Col and Wasp proteins from the different viruses whereas Cah and Hexon share similar structures.

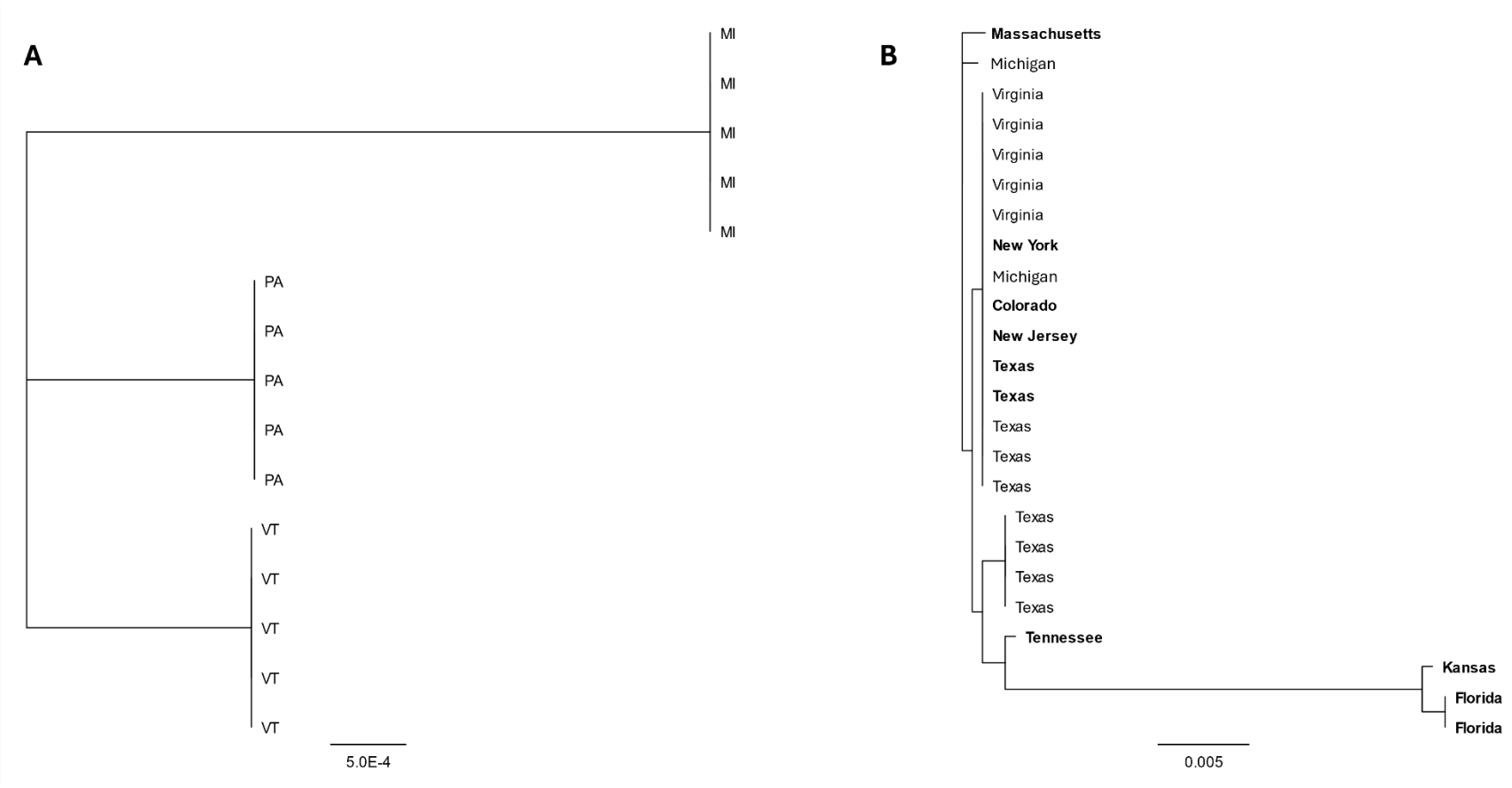

Fig 7. Neighbor joining trees depicting the relationships between partial sequences RepE1 of MdA-1 (A) and MnA-1 (B) from bass sampled from different locations in the United States. Samples identified in bold were collected from largemouth bass maintained in Bass Pro Shop live exhibits.

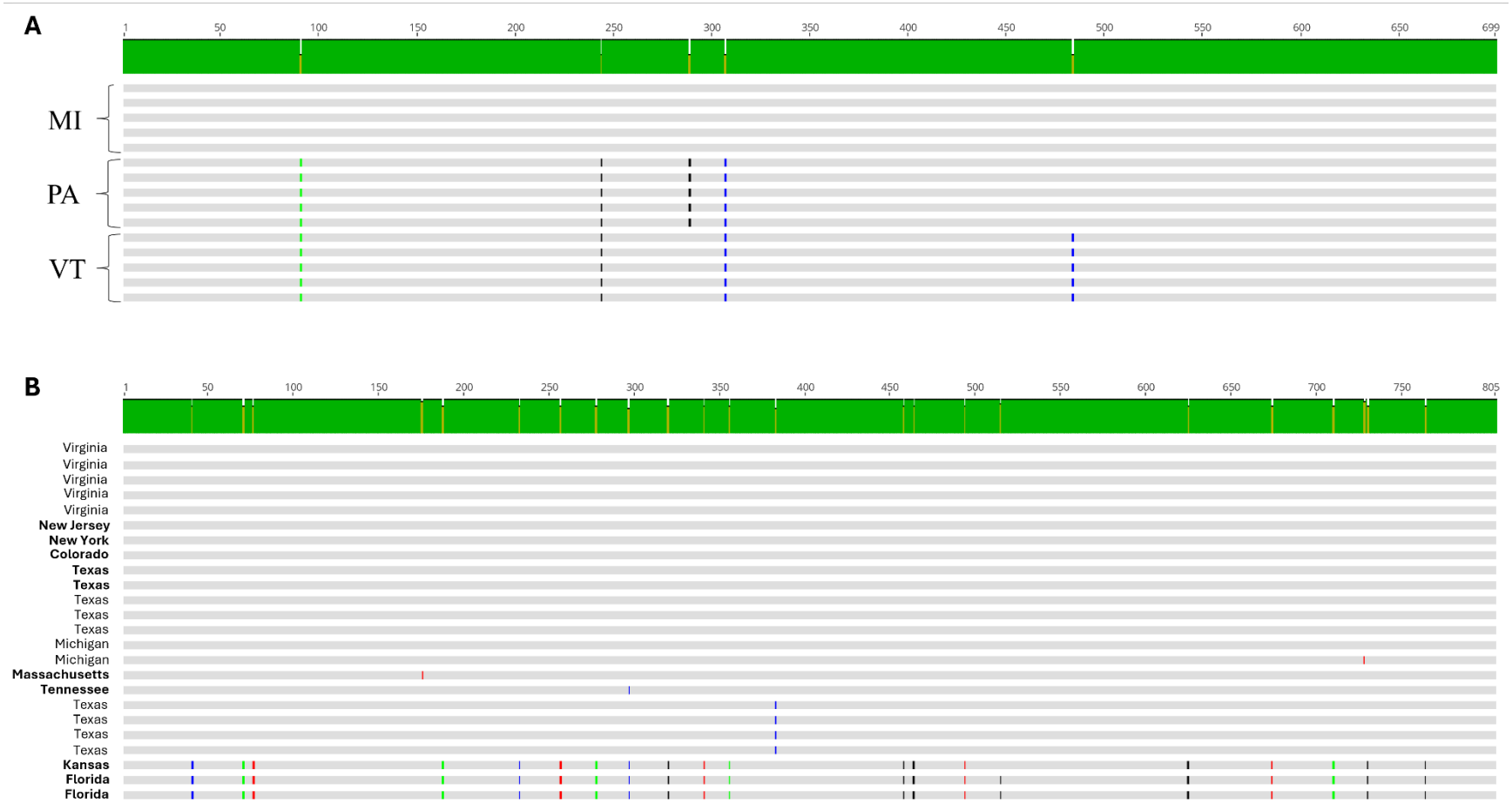

Fig 8. Alignment of RepE1 nucleotide sequences from samples collected from smallmouth bass (A) inhabiting waterbodies in Lake St Clair, MI; Susquehanna River, PA, and Lake Champlain (VT) or largemouth bass (B) represented in Figure 7A or 7B, respectively. Single nucleotide polymorphisms are identified in color to identify the base. Black = G, blue = C, green = A, red = T. Samples identified in bold were collected from largemouth bass maintained in Bass Pro Shop live exhibits

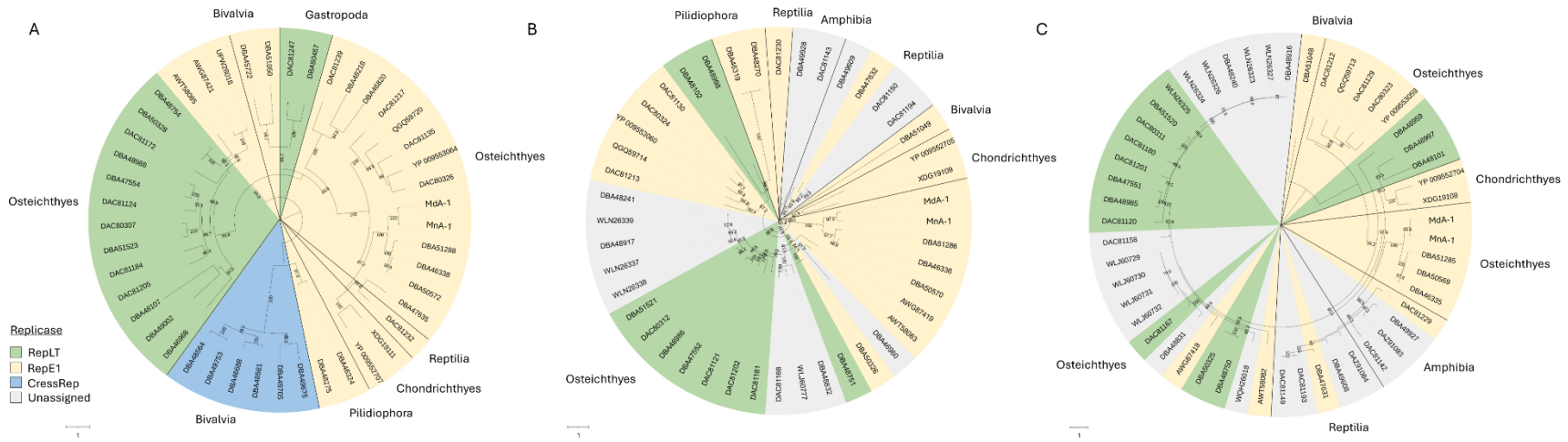

Fig 9. Circular maximum likelihood trees of replicase (A), adenain (B) and hexon (C) proteins of adomaviruses. Colors represent the replicase type. Class of the host organism is indicated along the margins of the tree. Bootstrap values are indicated for all branches where support is >75%.

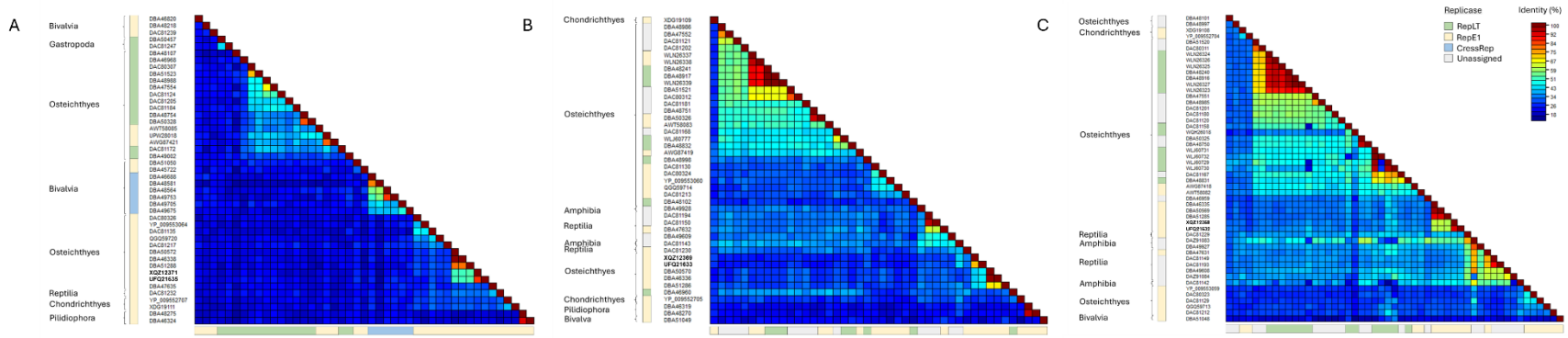

Fig 10. Pairwise protein identity matrix of replicase (A), adenain (B) and (C) hexon proteins. Replicase type is indicated along the margins as well as the Linnean class of the host organism. If known the replicase-type of each virus is indicated.

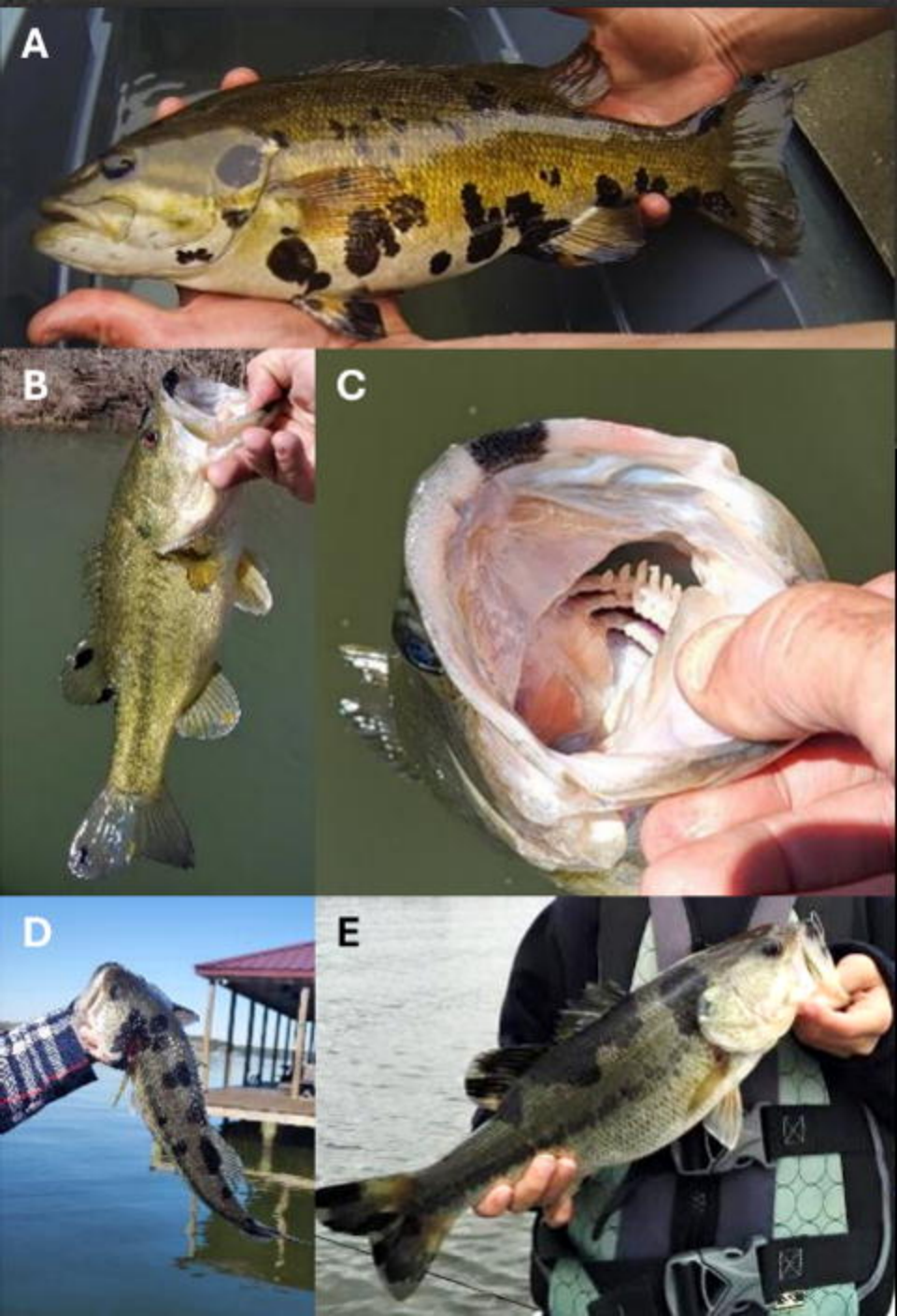
A
B
C
D
E

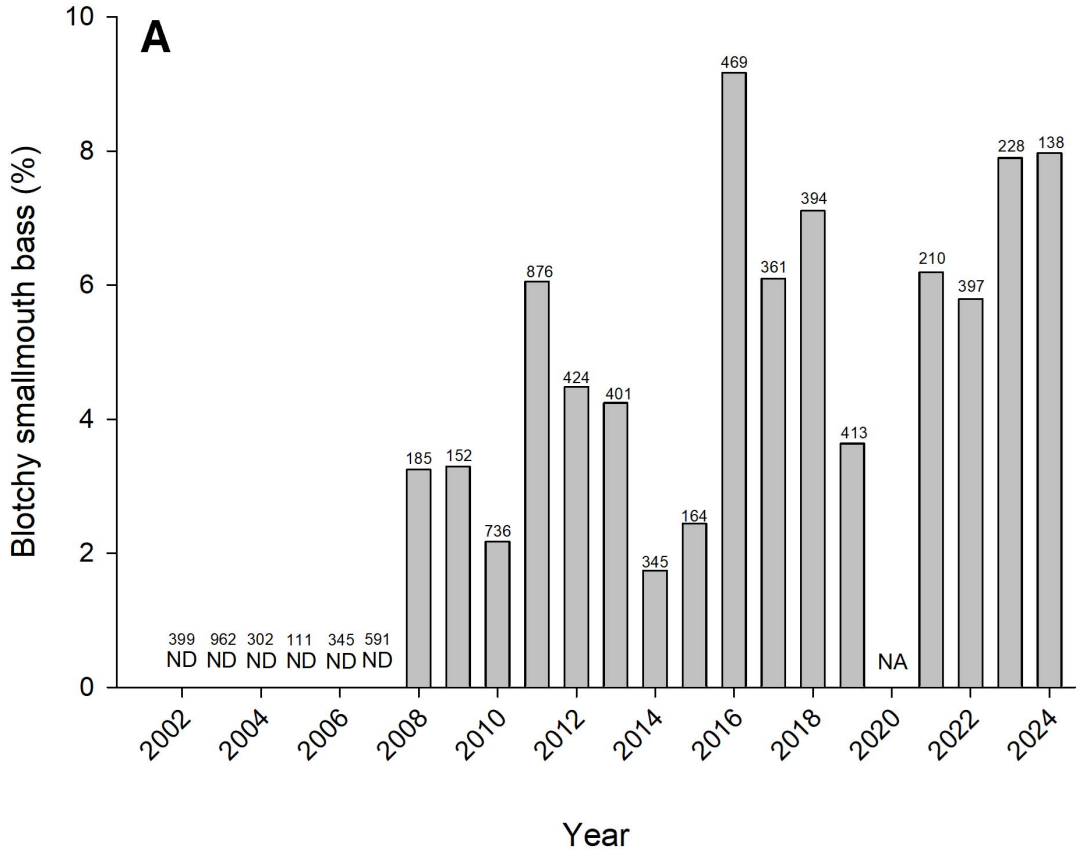
A
Blotchy smallmouth bass (%)
Year
0
2
4
6
8
10
2002
2004
2006
2008
2010
2012
2014
2016
2018
2020
2022
2024
399 ND
962 ND
302 ND
111 ND
345 ND
591 ND
185
152
736
876
424
401
345
164
469
361
394
413
NA
210
397
228
138

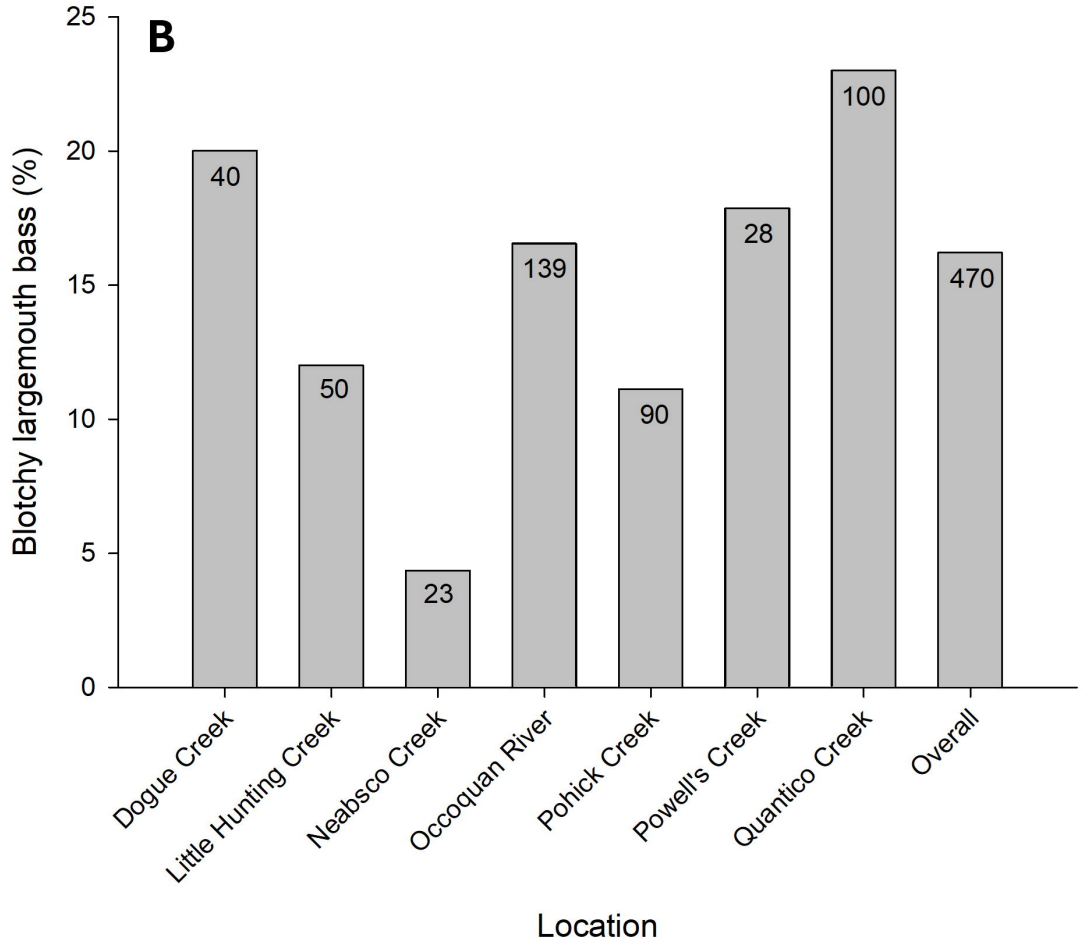
B
Blotchy largemouth bass (%)
Location
0
5
10
15
20
25
Dogue Creek
Little Hunting Creek
Neabsco Creek
Occoquan River
Pohick Creek
Powell's Creek
Quantico Creek
Overall
40
50
23
139
90
28
100
470

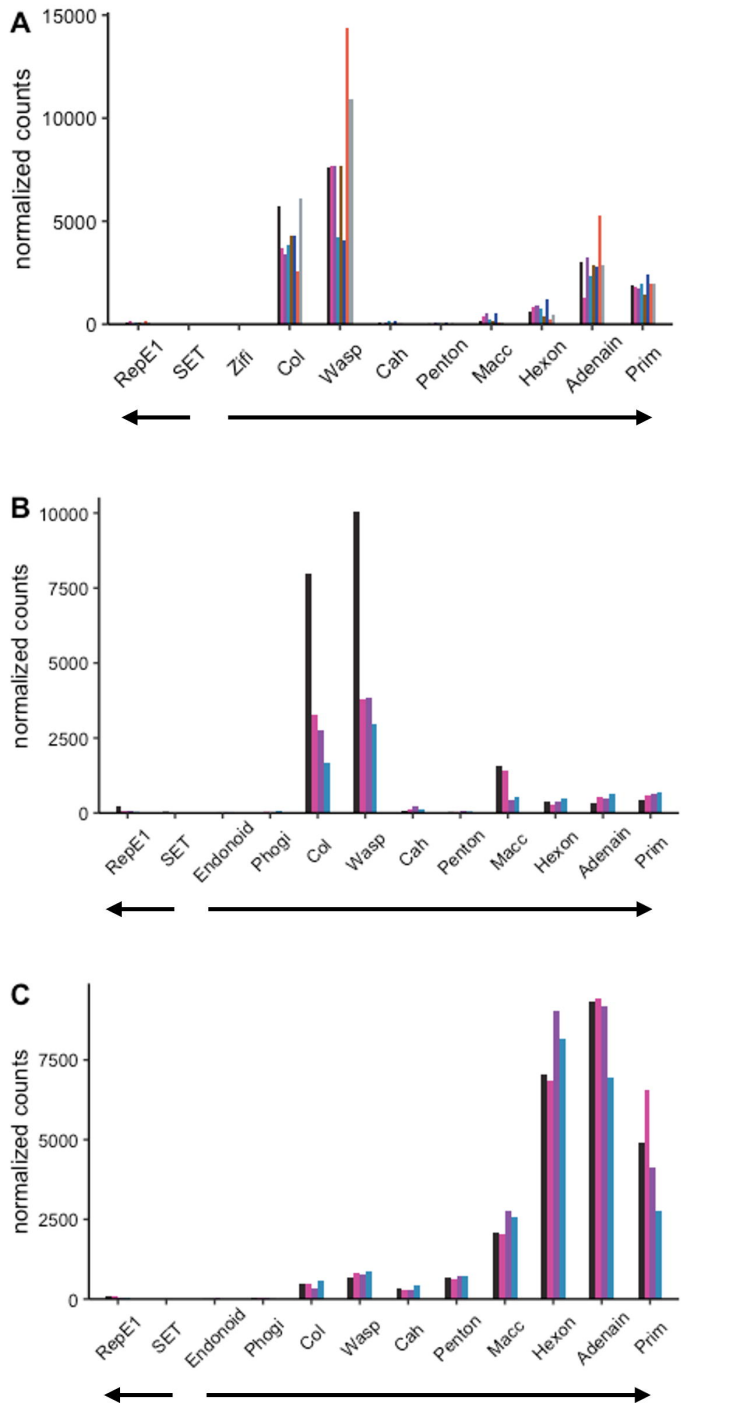
A
normalized counts
15000
10000
5000
0
RepE1
SET
Zifi
Col
Wasp
Cah
Penton
Macc
Hexon
Adenain
Prim
B
normalized counts
10000
7500
5000
2500
0
RepE1
SET
Endonoid
Phogi
Col
Wasp
Cah
Penton
Macc
Hexon
Adenain
Prim
C
normalized counts
7500
5000
2500
0
RepE1
SET
Endonoid
Phogi
Col
Wasp
Cah
Penton
Macc
Hexon
Adenain
Prim

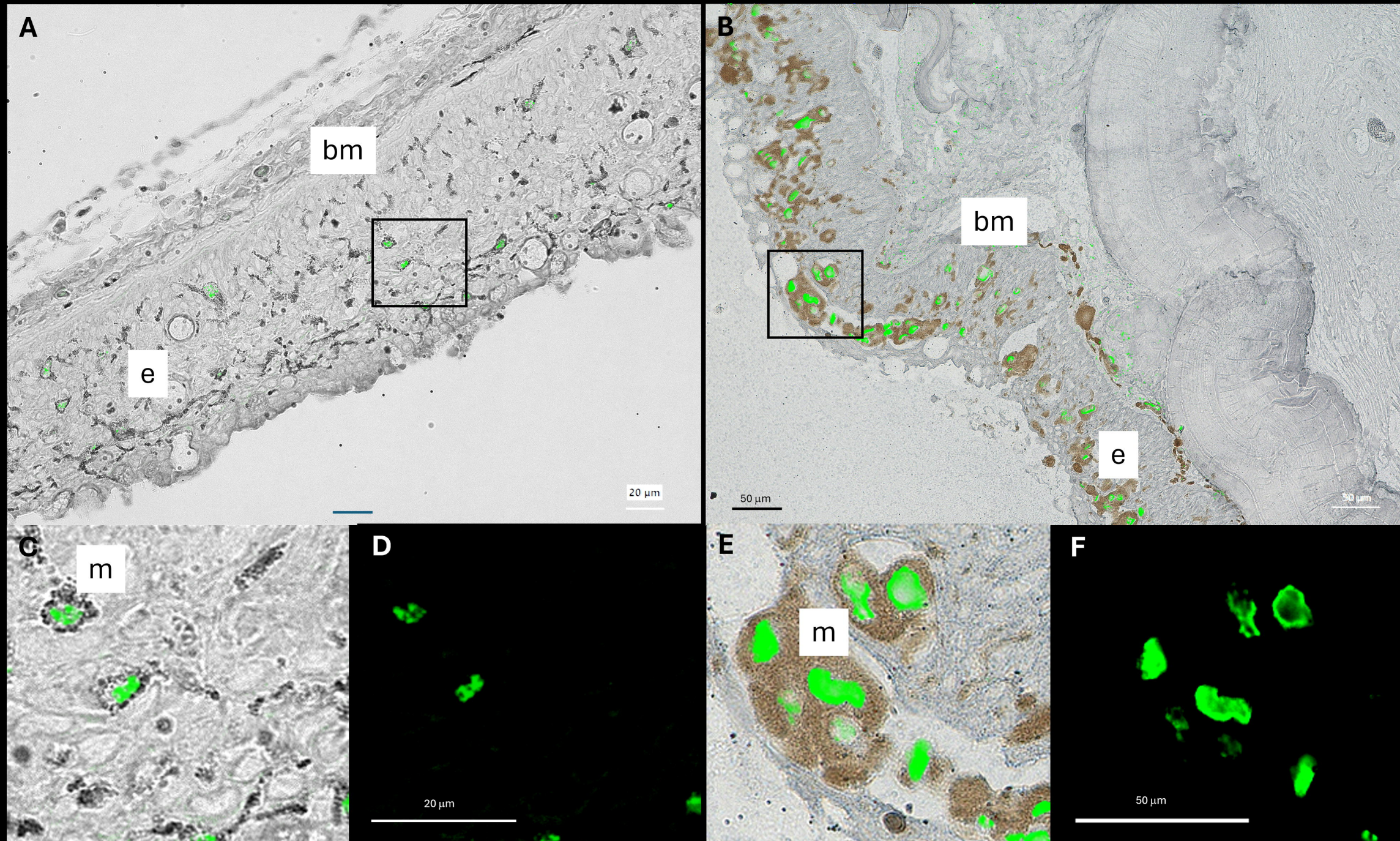
A
bm
e
20 µm
B
bm
e
50 µm
C
m
D
20 µm
E
m
F
50 µm

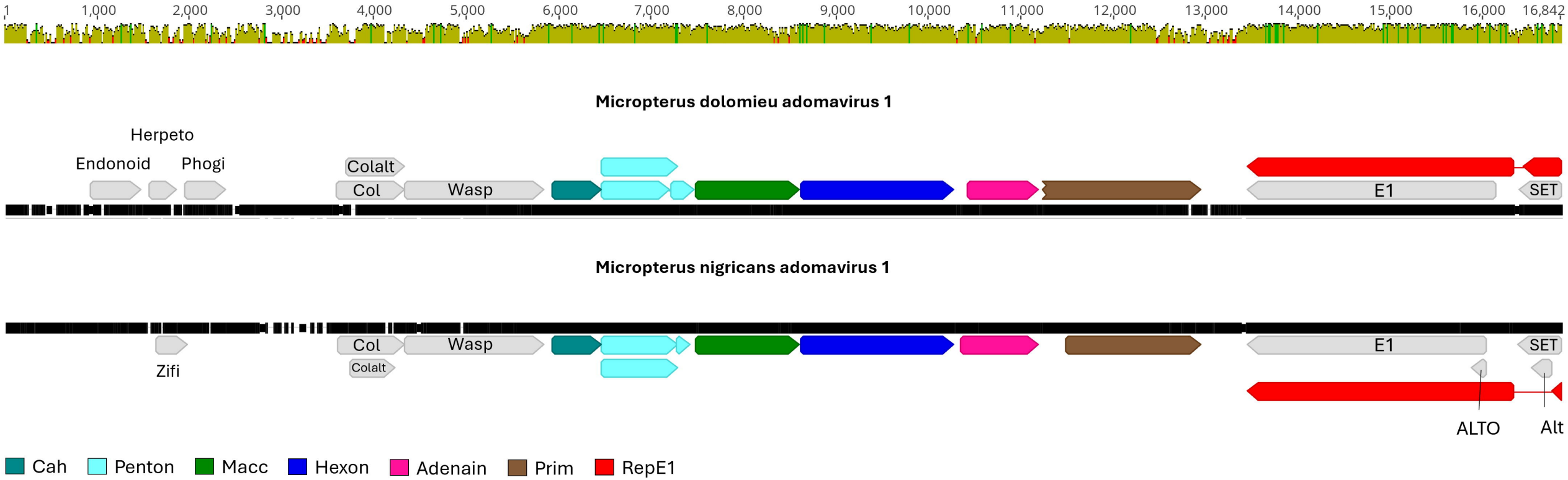
1
1,000
2,000
3,000
4,000
5,000
6,000
7,000
8,000
9,000
10,000
11,000
12,000
13,000
14,000
15,000
16,000
16,842
Micropterus dolomieu adomavirus 1
Herpeto
Endonoid
Phogi
Colalt
Col
Wasp
E1
SET
Micropterus nigricans adomavirus 1
Zifi
Col
Colalt
Wasp
E1
SET
ALTO
Alt
Cah
Penton
Macc
Hexon
Adenain
Prim
RepE1

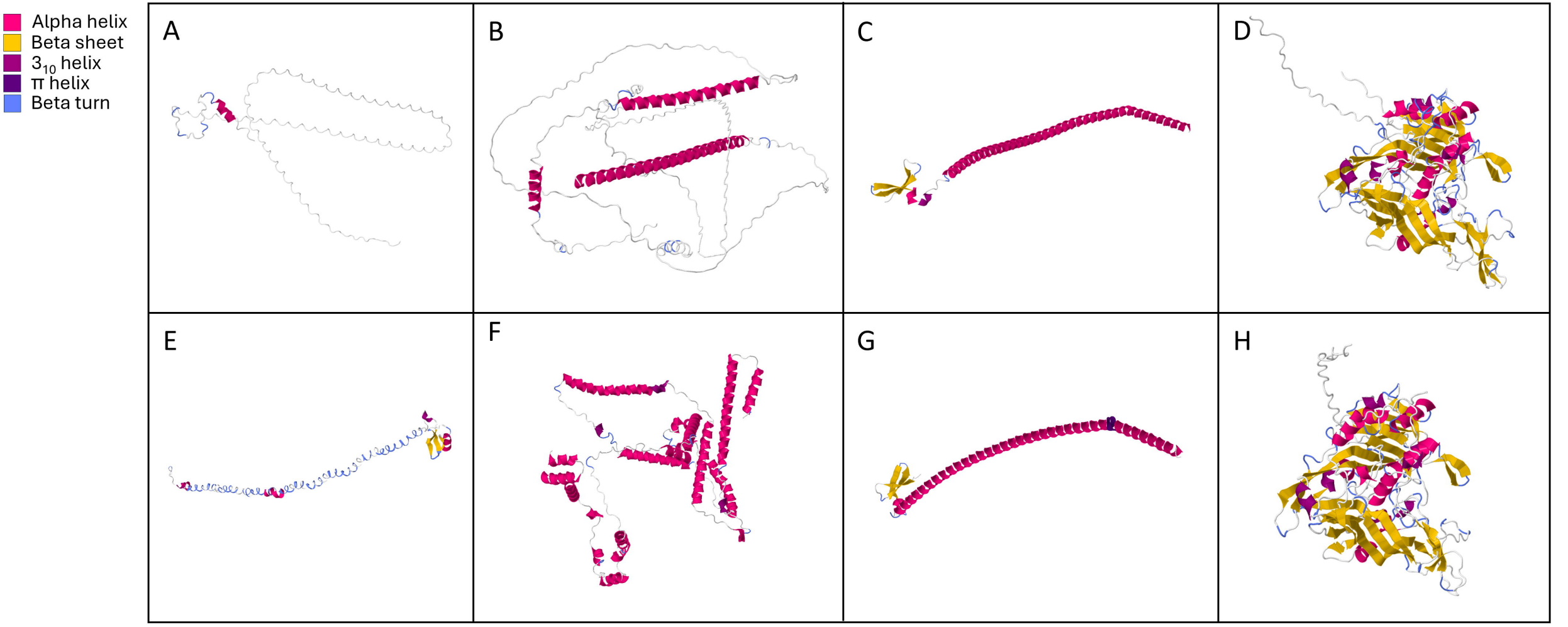
Alpha helix
Beta sheet
3_{10} helix
π helix
Beta turn
A
B
C
D
E
F
G
H

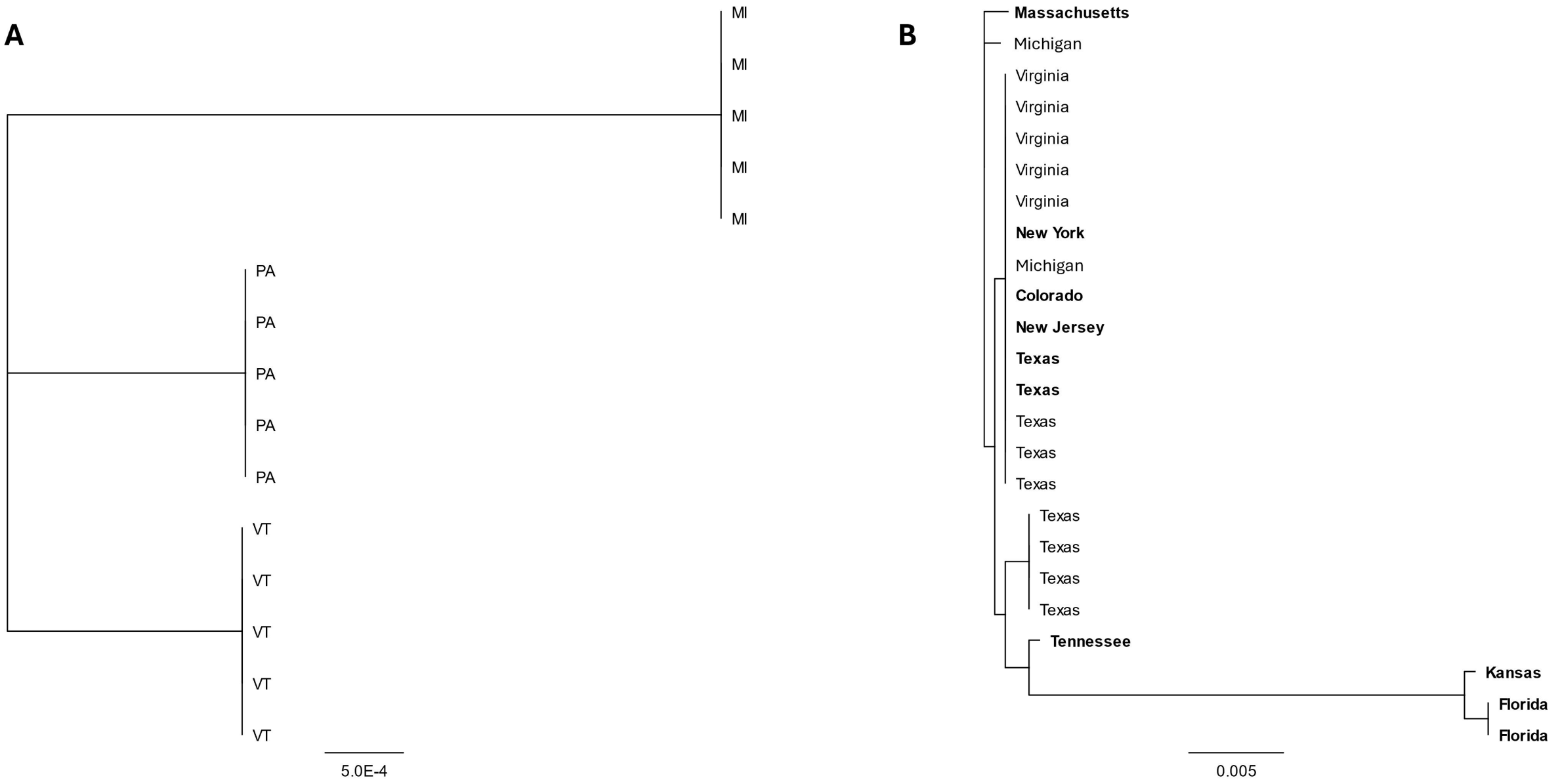
A
MI
MI
MI
MI
MI
PA
PA
PA
PA
PA
VT
VT
VT
VT
VT
5.0E-4
B
Massachusetts
Michigan
Virginia
Virginia
Virginia
Virginia
Virginia
New York
Michigan
Colorado
New Jersey
Texas
Texas
Texas
Texas
Texas
Texas
Texas
Texas
Texas
Tennessee
Kansas
Florida
Florida
0.005

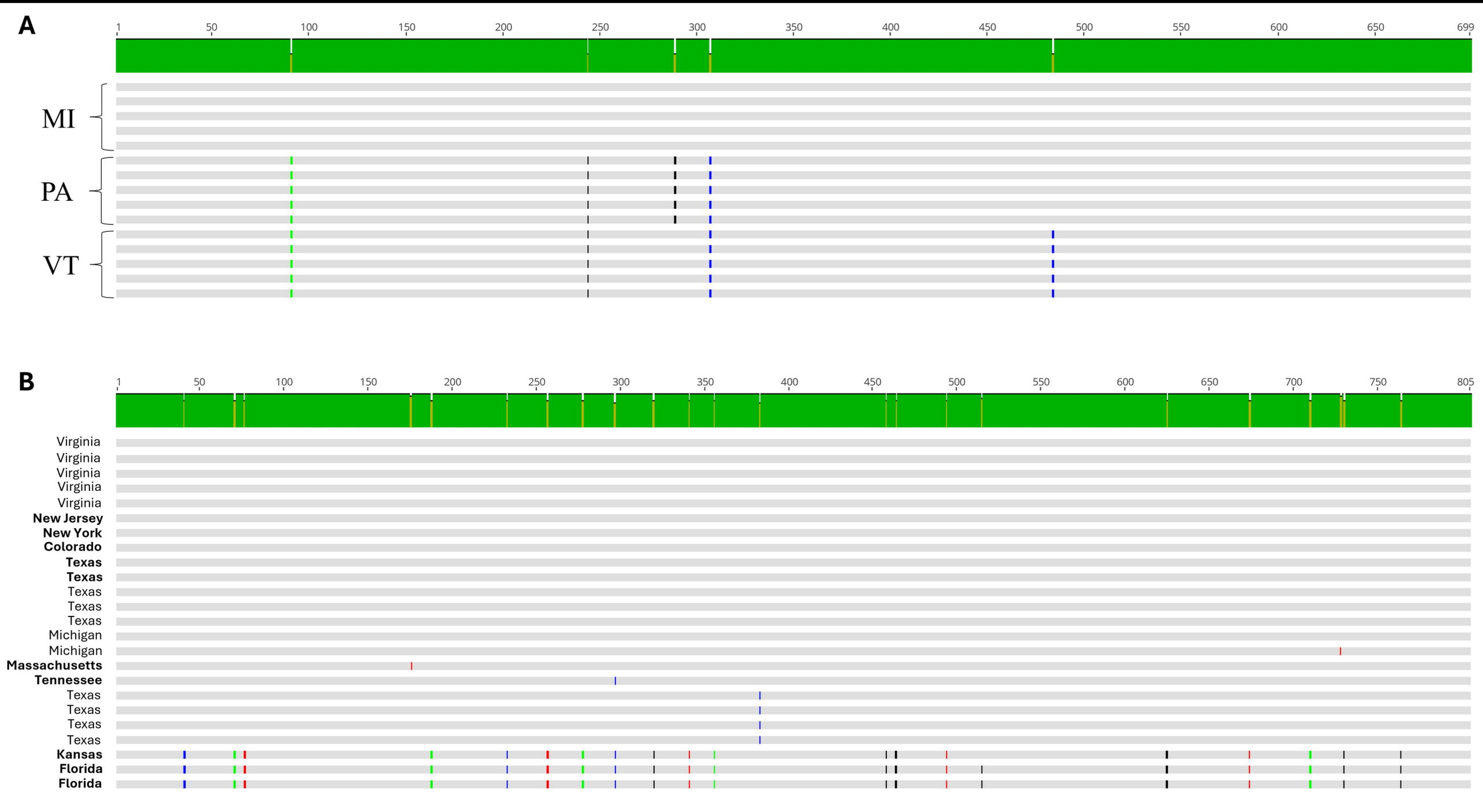
A
1
50
100
150
200
250
300
350
400
450
500
550
600
650
699
MI
PA
VT
B
1
50
100
150
200
250
300
350
400
450
500
550
600
650
700
750
805
Virginia
Virginia
Virginia
Virginia
Virginia
New Jersey
New York
Colorado
Texas
Texas
Texas
Texas
Texas
Michigan
Michigan
Massachusetts
Tennessee
Texas
Texas
Texas
Texas
Kansas
Florida
Florida

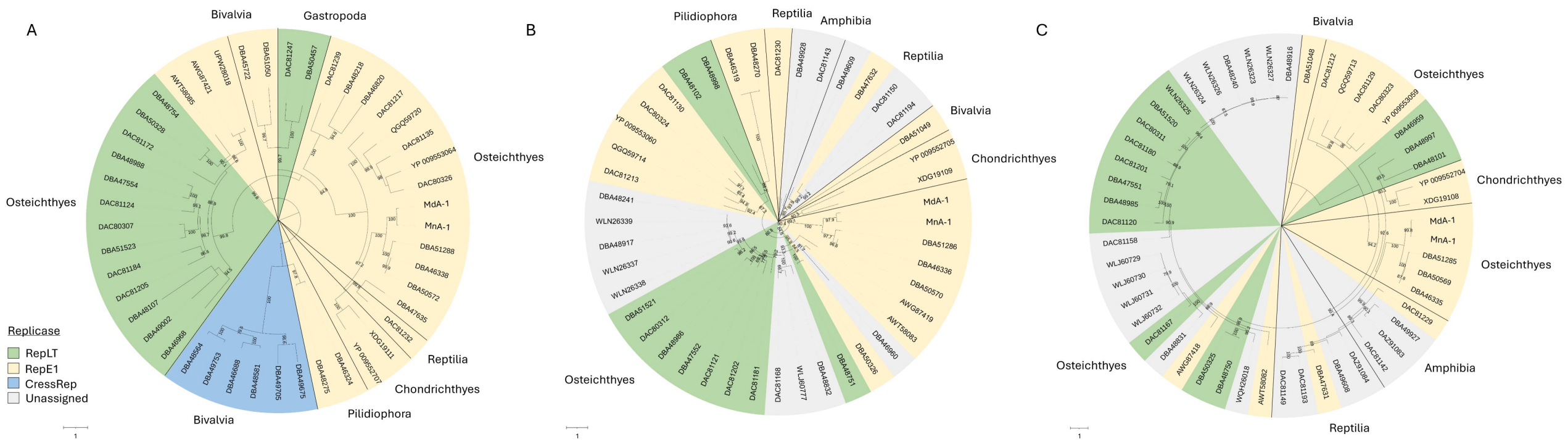
A
Bivalvia
Gastropoda
Osteichthyes
Osteichthyes
Reptilia
Chondrichthyes
Pilidiophora
Bivalvia
Replicase
RepLT
RepE1
CressRep
Unassigned
1
B
Pilidiophora
Reptilia
Amphibia
Reptilia
Bivalvia
Chondrichthyes
Osteichthyes
1
C
Bivalvia
Osteichthyes
Chondrichthyes
Osteichthyes
Amphibia
Reptilia
Osteichthyes
1

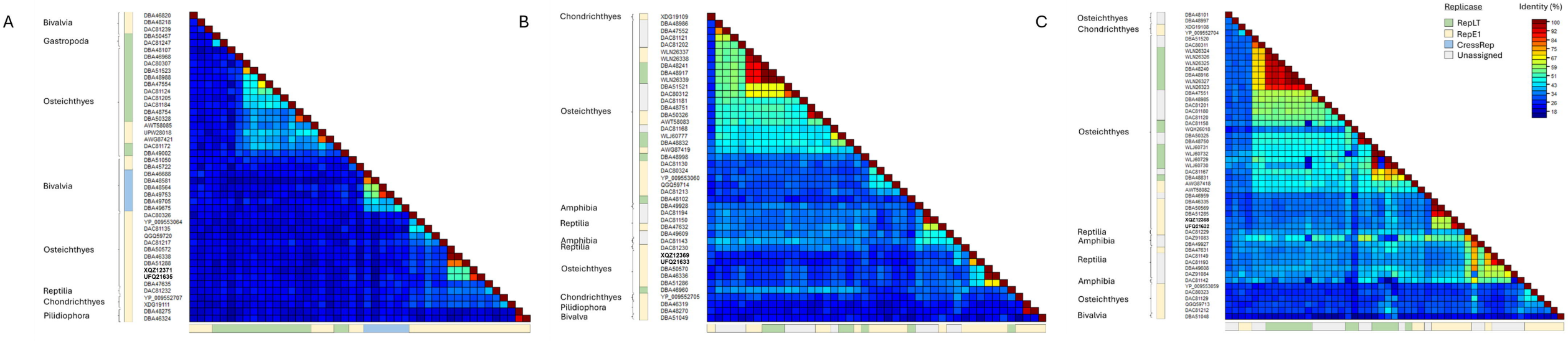
A
Bivalvia
Gastropoda
Osteichthyes
Bivalvia
Osteichthyes
Reptilia
Chondrichthyes
Pilidiophora
DBA46820
DBA48218
DAC81239
DBA50457
DAC81247
DBA48107
DBA46968
DAC80307
DBA51523
DBA48988
DBA47554
DAC81124
DAC81205
DAC81184
DBA48754
DBA50328
AWT58085
UPW28018
AWG87421
DAC81172
DBA49002
DBA51050
DBA45722
DBA46688
DBA48581
DBA48564
DBA49753
DBA49705
DBA49675
DAC80326
YP_009553064
DAC81135
QGQ59720
DAC81217
DBA50572
DBA46338
DBA51288
XQZ12371
UFQ21635
DBA47635
DAC81232
YP_009552707
XDG19111
DBA48275
DBA46324
B
Chondrichthyes
Osteichthyes
Amphibia
Reptilia
Amphibia
Reptilia
Osteichthyes
Chondrichthyes
Pilidiophora
Bivalva
XDG19109
DBA48986
DBA47552
DAC81121
DAC81202
WLN26337
WLN26338
DBA48241
DBA48917
WLN26339
DBA51521
DAC80312
DAC81181
DBA48751
DBA50326
AWT58083
DAC81168
WLJ60777
DBA48832
AWG87419
DBA48998
DAC81130
DAC80324
YP_009553060
QGQ59714
DAC81213
DBA48102
DBA49928
DAC81194
DAC81150
DBA47632
DBA49609
DAC81143
DAC81230
XQZ12369
UFQ21633
DBA50570
DBA46336
DBA51286
DBA46960
YP_009552705
DBA46319
DBA48270
DBA51049
C
Osteichthyes
Chondrichthyes
Osteichthyes
Reptilia
Amphibia
Reptilia
Amphibia
Osteichthyes
Bivalvia
Replicase
RepLT
RepE1
CressRep
Unassigned
Identity (%)
100
92
84
75
67
59
51
43
34
26
18
DBA48101
DBA48997
XDG19108
YP_009552704
DBA51520
DAC80311
WLN26324
WLN26326
WLN26325
DBA48240
DBA48916
WLN26327
WLN26323
DBA47551
DBA48985
DAC81201
DAC81180
DAC81120
DAC81158
WQH26018
DBA50325
DBA48750
WLJ60731
WLJ60732
WLJ60729
WLJ60730
DAC81167
DBA48831
AWG87418
AWT58082
DBA46959
DBA46335
DBA50569
DBA51285
XQZ12368
UFQ21632
DAC81229
DAZ91083
DBA49927
DBA47631
DAC81149
DAC81193
DBA49608
DAZ91084
DAC81142
YP_009553059
DAC80323
DAC81129
QGQ59713
DAC81212
DBA51048